SAPIENZA
UNIVERSITA` DI ROMA

Dottorato di ricerca in medicina sperimentale
XXX ciclo

"Mitochondrial-DAMPs released after Lung Transplantation promote Primary Graft Dysfunction"

Dottorando
Dott. Davide Scozzi

Docente Guida
Prof. Salvatore Mariotta

Coordinatore del dottorato

Prof. ssa Mara Torrisi

Anno Accademico 2016-2017

TABLE OF CONTENTs

LIST OF FIGUREs

1. Introduction

3. Material and Methods

4. Results

Abbreviations

AA	Arachidonic Acid
AIF	Apoptosis Inducing factors
ALI	Acute Lung Injury
ARDS	Acute Respiratory Distress Syndrome
BAL	Bronchoalveolar Lavage
BOS	Bronchiolitis Obliterans Syndrome
CG	Cathepsin G
CF	Cystic Fibrosis
COPD	Chronic Obstructive Pulmonary Disease
COX	Cyclooxygenase
CPB	Cardio-Pulmonary Bypass
DAMP	Damage associated molecular pattern
DPI	Difenilen Iodonio
ECMO	Extra-Corporeal Membrane Oxygenation
ERK 1/2	Extracellular Signal Related Kinases 1 and 2
FPR1	Formylated Peptide Receptor 1
G-CSF	Granulocyte-Colony Stimulating Factor
CGD	Chronic Granulomatous Disease
GPCR	Gi protein-coupled receptors

HA	Hyaluronan
HETE	Hydroxyeicosatetraenoic Acid
HMGB1	High Mobility Group Box 1
ICU	Intensive Care Unit
ISHLT	International Society for Heart and Lung Transplantation
IPF	Idiopathic Pulmonary Fibrosis
IRI	Ischemia Reperfusion Injury
5-LO	5-Lipoxygenase
LTB4	Leukotriene B4
LTx	Lung Transplantation
MAPK	Mitogen-Activated Protein Kinase
MPO	Myeloperoxidase
Mt-DAMPs	Mitochondrial Damage Associated Molecular Pattern
Mt-DNA	Mitochondrial DNA
NADPH	Nicotinamide adenine dinucleotide phosphate
NE	Neutrophil Elastase
NO	Nitric Oxide
NETs	Neutrophil Extracellular traps
PAMP	Pathogen Associated Molecular Pattern
PAH	Pulmonary Arterial Hypertension
PEEP	Positive End Expiratory Pressure
P/F	PaO2/FiO2
PI3K	PhosphatIdylinositol-3-Kinase
PGs	Prostaglandins
PGD	Primary Graft Disease
PLA 2	Phospholipase A 2
PKC	Protein Kinase C
PMA	Phorbol-12-myristate-13-acetate
PR3	Proteinase 3
PRR	Pathogen Recognize Receptor
PSGL1	P-selectin Glycoprotein Ligand 1

ROS	Reactive Oxygen Species
SLT	Single Lung Transplant
TLR	Toll-Like Receptor
VILI	Ventilator Induced Lung Injury
XDH	Xanthine Dehydrogenase
XO	Xanthine Oxidase

Abstract

Lung transplantation (LTx) often results in primary graft dysfunction (PGD), a form of acute lung injury (ALI) that is responsible for poor short and long-term outcomes. Although the underlying mechanisms that promote PGD are undefined recent evidence has pointed to the involvement of danger associated molecular patterns (DAMPs). Mitochondrial DAMPs (Mt-DAMPS) share the potent immunostimulatory qualities of bacterial pathogen-associated molecular patterns (PAMPs) since they can activate the necrotactic formyl peptide receptor 1 (FPR1) regulating neutrophil migration to injured areas. However, the contribution of the Mt-DAMPs-FPR1 axis to organ transplant injury remains unclear.

In a murine orthotopic LTx model of PGD, we detected the release of donor-derived Mt-DAMPs into the injured airways. We also demonstrate that FPR1 expression in the recipient regulates neutrophil intragraft distribution by promoting airways neutrophilia. This effect seems to be specifically associated with the activation of the Mt-DAMPs-FPR1 axis which leads to neutrophil upregulation of adhesion molecules and increased extravascular neutrophil cluster stability. As a consequence of FPR1 expression, we demonstrated prolonged neutrophil retention into the injured airways and exacerbation of the ALI. In a prospective study of 62 human lung recipients, circulating Mt-DAMPs, in the form of mitochondria DNA (Mt-DNA), were increased after LTx and the higher perioperative levels were predictive of severe late PGD.

In conclusion, this thesis proposes that the early release of graft-derived Mt-DAMPs after LTx contributes to exacerbating ALI through an FPR1 dependent regulation of neutrophil intragraft trafficking and activation. Moreover, higher perioperative circulating

levels of Mt- DNA in human LTx recipients appear to be a possible biomarker for the early detection of severe PGD.

1. Introduction

The history of LTx began during the 1940s and 1950s with the pioneering animal experimentation by Vladimir Demikhov and Henry Metra that demonstrated the technical feasibility of this procedure. However, it was only in 1963 that James Hardy performed the first human LTx at the University of Mississippi. From 1963 to 1978, multiple attempts at LTx failed mostly because of rejection and problems with anastomotic bronchial healing. However, since the introduction of the heart-lung machine, coupled with the development of immunosuppressive drugs, LTx finally became a valid therapeutical option.

Today LTx is considered a well-established live-saving treatment especially for selected patients with end-stage lung disease such as Chronic obstructive pulmonary disease (COPD), idiopathic pulmonary fibrosis (IPF), cystic fibrosis (CF), alpha1-antitrypsin disease and primary pulmonary hypertension. However, although LTx is a valuable option for advanced pulmonary diseases, still the rate of complication, especially in the early Post-Operative phase, remain considerably high.

1.1 Primary Graft Dysfunction

PGD is a form of ALI that develops in the first hours to days after LTx. Historically, PGD has been variously referred to as primary graft failure, ischemia-reperfusion injury (IRI), re-implantation edema, allograft dysfunction, and pulmonary reimplantation response [1-3]. This lack of standard definitions and diagnostic criteria has been responsible for the conflicting results regarding incidence and mortality reported in the past literature and contributed to the relatively poor insight in the cellular and molecular mechanisms beyond its pathophysiology. For these specific reasons, the International

Society for Heart and Lung Transplantation (ISHLT) standardized in 2005 the definition of PGD as a condition occurring within 72 hours after LTx and characterized by the presence of severe hypoxemia, lung edema, and the radiographic appearance of diffuse pulmonary opacities without other identifiable cause [4]. A grading system based on PaO_2/FIO_2 (P/F ratio) and the chest x-ray appearance was also proposed to stage the severity of PGD **(figure 1.1)**. According to this system, patients should be evaluated as to their grade immediately postoperatively (T0), at 24 hours (T24), 48 hours (T48), and 72 hours (T72). Based on this new definition it has been possible to identify a severe form of PGD (grade 3) which is associated with higher 30-day mortality and more significant alteration in plasma markers of lung injury compared to those with lower grades [5].

Grade at T0, T24,T48,T72	Radiographic diffuse pulmonary opacities	PaO2/FiO2	Specific exceptions
0	no	Any	
1	yes	>300	On nasal cannula of FiO2<0.3
2	yes	200-300	
3	yes	<200	Any patients on ECMO or NO with FiO2>0.5MV

Fig. 1.1 ISHLT 2005 definition and grading system for PGD.

1.1.1 Epidemiology

PGD is the most common complication after LTx with a frequency that varies from 11% to 57% according to the past literature [3]. However, since the ISHLT 2005 standardized definition and grading system, the incidence of severe PGD (Grade 3) at T48-72 has been reported to be about 10-25% with a variability likely dependent on differences in institutional practices and risk factors distribution [5-11]. PGD is the leading cause of early death after LTx with 30-day mortality close to 50% for the most severe forms [12]. PGD also significantly impact morbidity resulting in longer duration of mechanical ventilation, longer intensive care unit (ICU)/hospital stay, increased costs and an overall protracted and often compromised recovery of the lung function among survivors [13]. To this hand, a retrospective cohort study including 255 consecutive LTx procedures [2] shows how survivors of T72 Grade 3 PGD at 12 months cover far less distance as measured by 6-minute walk distance than those without Grade 3 PGD.

Finally, PGD long-term survivors have an increased risk (RR 1.73-2.53) of developing bronchiolitis obliterans syndrome (BOS) which is independent of the concurrent incidence of acute rejection, lymphocytic bronchitis, and community-acquired respiratory viral infections [9]. The increased markers of epithelial injury recently described in PGD patients and associated with BOS seem to indicate a possible link between the degree of ALI and the aberrant inflammation which can lead to BOS [14].

1.1.2 Risk Factors

Risk factors for PGD can be related to donor and recipient characteristics and the perioperative management. Despite the fact that specific donor characteristics, identified

as possible risk factors for PGD, vary somewhat among studies, smoking history and the donor age (over 45 or under 21) are commonly associated with a significantly increased risk for PGD [15]. Female gender and an African-American donor are also variables related to the PGD development [16].

Several independent recipient variables associated to PGD have been recently described in a multicenter prospective cohort study enrolling 1255 LTx patients [6]. Among these, age, female gender, African-American and overweight or obese recipient body habitus appeared to be the most significant. On the other hand, the underlying lung disease that led to the need for LTx may also influence the risk of PGD. A recipient diagnosis of sarcoidosis or pulmonary arterial hypertension (PAH) has been shown to be associated with higher PGD frequency [17]. Patients with pulmonary fibrosis and elevated pulmonary artery pressures before LTx also have an increased risk of PGD [18]. However, the association between recipient lung disease and the risk of developing PGD is unfortunately confounded by the variable use of cardiopulmonary bypass (CBP) during LTx based upon the underlying indication. (i.e., the extended use of CBP in patients with pulmonary arterial hypertension). Other identified risk factor related to the surgical procedure and perioperative management is represented by a single lung transplant (SLT), large-volume of blood product transfusion and high FIO2 during reperfusion [6].

Besides donor and recipient variables there are also several factors related to the organ procurement, storage, and reperfusion that may contribute to lung injury. The neurogenic hypotension, impaired endocrine function (i.e., diabetes insipidus), and the release of pro-inflammatory cytokine typical of the Brain-Death condition are in fact altogether responsible for an increased risk of PGD after LTx [19]. Also, ventilator-

associated lung injury due to alveolar over-distension before to lung retrieval also represents a factor which can facilitate the development of PGD [20].

1.1.3 Pathogenesis

PGD is the result of several injuries inflicted to the donor's lung before the transplant (retrieval, preservation, implantation, and reperfusion) and by other factors such as acid aspiration, pneumonia, and microtrauma from mechanical ventilation which may occur after the surgical procedure [1]. Among these events, the IRI plays the major contribution to PGD development promoting endothelial and parenchymal cell death and activating the immune response to the graft **(Fig. 1.2)**.

Ischemia is a necessary condition for solid organ transplantation and is characterized by a combination of hypoxia and mechano-transduction deficiencies in the arterioles and capillaries. This particular condition can trigger endothelial cells and macrophages activation [21].

Hypoxia involves two fundamental molecular events in ischemic tissue:

1. The decrease of the intracellular ATP and its progressive conversion into AMP along with the subsequent end-products adenosine, inosine, and hypoxanthine [22].
2. The activation of a calcium-dependent protease that converts tissue xanthine dehydrogenase from its D (XDH) form to its O (XO) form or xanthine oxidase.

   The XO directly uses oxygen as an electron acceptor. Although its substrate is present, the XO cannot work until the tissue remains ischemic. When the blood flow is restored, the presence of oxygen induces xanthine oxidase to convert hypoxanthine into uric acid generating superoxide $O2^-$ anion. From the conversion

of $O2^-$ by the superoxide dismutase (SOD) originates H2O2 which, in turn, can generate a very reactive species such as the hydroxyl radical • OH. An increased production of reactive oxygen species (ROS), which are already produced in small quantities under normal conditions, may also be triggered by electron flow recovery along the respiratory chain occurring with the resumption of respiration in mitochondria. Each of these oxidizing agents can, in turn, trigger chain reactions, (i.e. lipo-oxidation of cell membranes), with severe consequences regarding cell damage and tissue injury [23].

Mitochondria damaged by ischemic injury significantly contribute to the oxidative stress occurring during reperfusion. Damage to mitochondrial membrane (caused by phospholipases), results in malfunction of the electron transport chain which leads to increased mitochondrial instability. As a result, ROS production is increased while ATP synthesis is reduced. These events promote the formation of mitochondrial permeability transition pores and lead to the initiation of the intrinsic apoptosis pathway [24].

Some evidence also reveals the role of nitric oxide (NO) produced by endothelial cells in response to ischemia. The NO reaction with $O2^-$ is extremely fast and leads to the formation of peroxynitrite, a potent oxidant which can directly activate the PARP-1 nuclear enzyme. PARP-1 activation, in turn, promotes the leakage of pro-apoptotic elements (AIF) from mitochondria facilitating programmed cell death [25].

Along with the reduced levels of intracellular ATP, the calcium homeostasis is also deregulated. During the ischemic phase, due to the ATP depletion, there is a progressive reduction in the functionality of the Na^+/K^+ ATPase pump. The levels of intracellular sodium rise leading to osmotic swelling. To prevent cellular swelling Ca^{++} is exchanged

with sodium through $2Na^{+}/Ca^{++}$exchangers. Following reperfusion, intracellular calcium overload is then exacerbated. Intracellular imbalances in Ca^{++} levels contribute to increasing mitochondria dysfunction favoring the irreversibility of the damage [24].

The vascular alterations occurring during ischemia mostly resemble what happens during an acute inflammatory process. The reduced availability of vasodilator NO in the microenvironment and the lack of mechanotransduction in arterioles and capillaries promote alterations in vascular tone and permeability, endothelial activation and expression of surface adhesion molecules that can recruit locally circulating leukocytes. These events lead to a progressive increase in the extravascular water content, which is increasingly marked especially as a result of the poor state of organ conservation or to a prolonged time of ischemia. The progressive compression of the capillaries then prevents a uniform distribution of blood flow in the periphery at re-infusion ("no reflow") further aggravating the cell damage caused by ischemia [26].

Re-establishing the perfusion of the ischemic tissue is necessary to maintain the vitality of the organ, but reperfusion itself can trigger a complex cascade of events characterized by increased microvascular permeability, increased pulmonary vascular resistance, pulmonary edema, compromise oxygenation and pulmonary hypertension [27].

Clinical and experimental evidence suggests that IRI follows biphasic kinetics [22, 28]. The early reperfusion phase, which mainly depends on the characteristics of the donor, and the delayed phase which occurs within 24 hours of reperfusion and depends primarily on the characteristics of the recipient. Resident macrophages and donor endothelial cells activated as a result of ischemic damage mediate the early phase while lymphocytes, but above all recipient neutrophils, are mainly involved in the late phase of reperfusion injury

[22]. Neutrophils represent the main infiltrating cellular subset which can be detected in the Bronchoalveolar Lavage (BAL) differential count early after LTx, and their level remains high during the next 2-4 weeks post-transplant [29]. Activated neutrophils are strongly associated with PGD since they can release chemotactic mediators by promoting an inflammatory environment. Also, the remarkable production of ROS mediated by the assembly of the Nicotinamide Adenine Dinucleotide Phosphate (NADPH) oxidase complex and the massive release of lithic enzymes contained in cytoplasmic granules by activated neutrophils contribute to the extension of the tissue damage during re-infusion [30]. Neutrophils can also promote inflammation through undergoing a unique form of programmed cell death termed "NETosis." In this regard, NETs have been reported in the Bronchoalveolar Lavage fluid (BALf) of human LTx recipients with PGD and in experimental LTx mouse models [31].

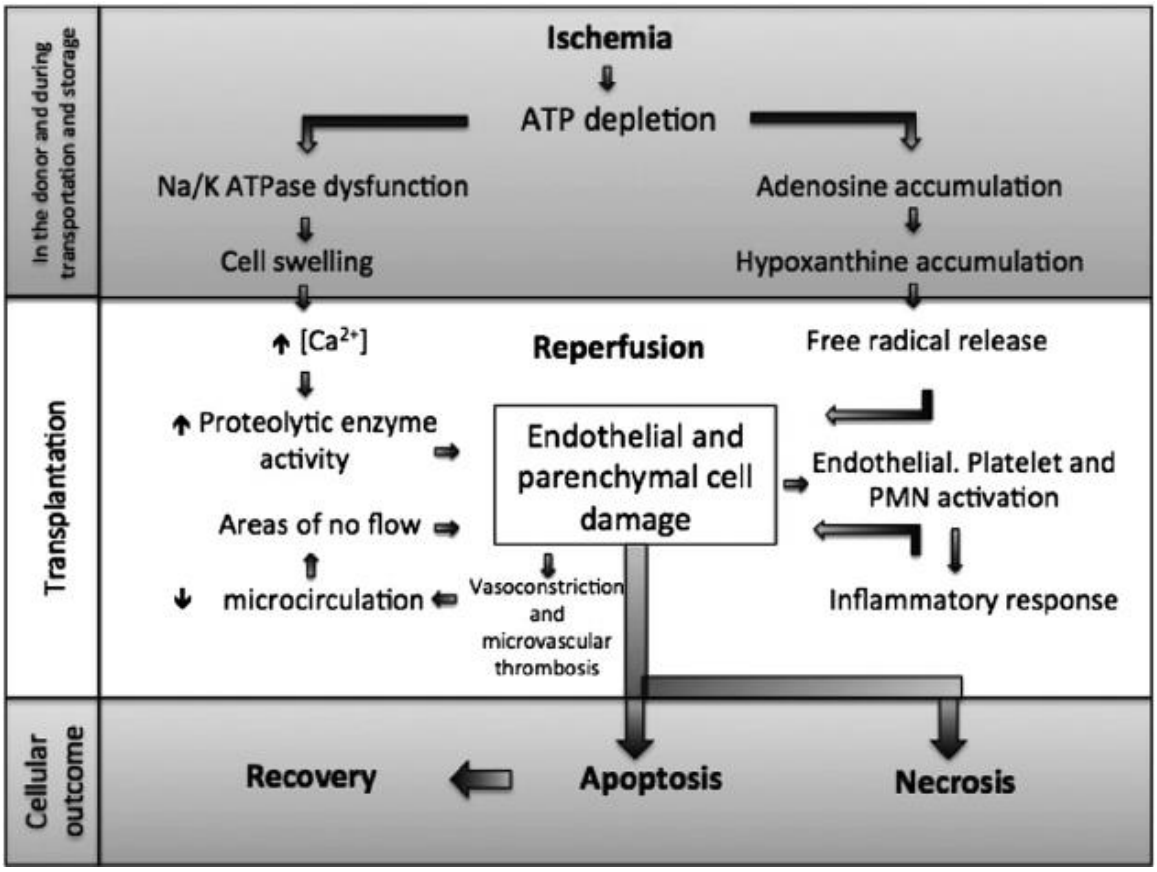

Fig. 1.2 Mechanisms of Ischemia-Reperfusion Injury [21].

A prolonged time of ischemia results in the depletion of the ATP levels, which is associated with the activation of intracellular pathways of damage. The accumulation of ATP intermediates and the reduction of the source of cellular energy lead to increase in oxidative stress, imbalances in the regulation of Ca^{++} homeostasis, predisposing to the activation of cell death programs. Reperfusion exacerbates the initial reversible cellular damage altering cellular metabolism and leading to the recruitment of inflammatory cells.

1.1.4 Clinical manifestation

PGD is a form of ALI related explicitly to LTx that occurs within the first 72 hours after the surgical procedure. PGD is characterized by diffuse alveolar damage and pulmonary edema that are clinically related to progressive hypoxemia, and radiographic pulmonary infiltrates without other identifiable causes [4]. This definition required the exclusion of other mechanical, immune and infectious causes that can mimic, modify, or even confound the PGD definition and grading. The ALI associated with PGD is generally progressive and includes a spectrum of severity which ranges from milder pulmonary edema to a more dramatic impairment of the lung function.

The extension of the pulmonary dysfunction is measured through the P/F ratio which should be ideally measured on a FiO_2 of 1.0 and a positive end-expiratory pressure (PEEP) of 5 cm H_2O. The radiographic findings of PGD **(Fig. 1.3)**, even if nonspecific, include perihilar ground-glass opacities, peribronchial and perivascular thickening, and reticular interstitial and airspace opacities predominantly located in the middle and lower lung lobes [32]. Parenchymal opacities usually appear on postoperative day 1, peak by day 3 and start to resolve on postoperative day 5-10; [33] However, the complete resolution is dependent on the severity of the initial injury and can take even few months among survivors [32]. Clinical improvement in the P/F ratio often precedes the radiographic resolution, and it poorly correlates with the radiographic findings. However, recent evidence suggests that different patterns of clinical resolution can also be related to the presence of various phenotypes of PGD [12].

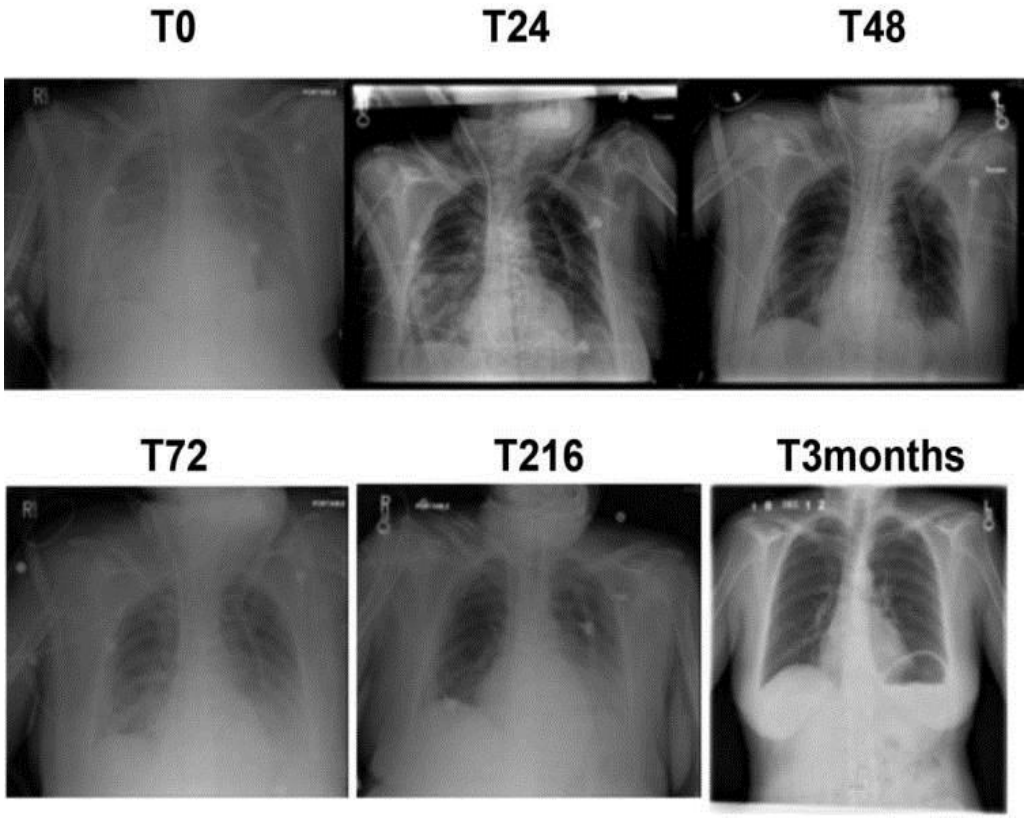

Fig. 1.3 Radiological progression of PGD [34]

Radiographic progression of severe grade 3 PGD (at T0, T24, T48, T72, T216 after extubation, and T3 months) after bilateral sequential LTx. 22-year-old donor from a motor vehicle accident. The recipient was a 62-year-old female with emphysema.

1.1.5 Treatment

The principles of PGD treatment are similar to those in acute respiratory distress syndrome (ARDS) and include lung protective mechanical ventilation and supportive therapies to reduce the secondary organ damage. Therapeutic options specifically directed to treat PGD are limited. Inhaled nitric oxide (iNO) has been proved beneficial since it can correct a ventilation-perfusion mismatch and, without affecting the systemic blood pressure, lowers the pulmonary artery pressure [35]. 10–20 ppm of iNO administration is currently recommended in stage 3 PGD patients with persistent hypoxemia and increased pulmonary artery pressure [36]. In severe PGD patients who failed to respond to all conventional treatments and iNO use, extracorporeal membrane oxygenation (ECMO) is used by many transplant centers as a last life-saving option [36]. Along with correcting PGD related hypoxia ECMO also protects the lungs from the potential harmful effects of aggressive mechanical ventilation reducing the occurrence of ventilator-induced lung injury (VILI) [37, 38]. Existing data regarding the best timing for this procedure show that ECMO should be performed within the first 24 hours from severe PGD detection [36].

Considering the limited options available to treat PGD patients most of the therapeutic efforts are currently directed to the prevention of IRI in the donor's lung. Various techniques for organ preservation have been developed over the last few years to reduce the risk of IRI. However, the most effective remain the control of the cold ischemia time. Although the most appropriate temperature and duration of cold ischemia is debated, most transplant centers store the organs at a temperature between 4°C and 8°C and consider an ischemia duration of up to 8 hours acceptable [39]. However, ischemia duration is generally evaluated along with the other risk factors in order to make a final transplant

decision [1]. The increased extravascular water content and interstitial edema, typically associated with IRI, is generally managed through the perfusion of the lungs with solutions containing high-oncotic compounds such as albumin, glucose, mannitol or dextran 40. Vascular tone alterations require the perfusion of the pulmonary circulation with vasodilatory drugs such as PGE-1 or prostacyclin even before withdrawal and subsequently after implantation of the transplanted organ. However, the best functional results are attributed to the perfusion of the low-pressure pulmonary circulation before withdrawal with a solution maintained at 4 degrees, a process called *pneumoplegia* [40].

Mechanical ventilation is also very important since evidence reveals that it may aggravate a pre-existing lung injury leading to a VILI [41]. A protective pressure-controlled mechanical ventilation in FiO_2 50%, with PEEP at 5 cm H_2O and airway peak pressure set at 20–25 cm H_2O is generally adopted for this reason. Also, to prevent barotraumas, some center previously provide continuous and gradual inflation to 20 cm H_2O to the lung allograft [42].

The reperfusion technique may also impact PGD risk. Experimental studies showed that the levels of pulmonary artery pressure are critical in the first 10 min of reperfusion [43-45]. For this reason, after the vascular anastomosis, the reperfusion clamp is gradually opened for a duration longer than 10 minutes.

Gene-based therapies have also been recently proposed in LTx in order to provide the allograft with potential resistance to the IRI. For example, in a single LTx model in rats, trans-tracheal administration of the gene coding for the anti-inflammatory cytokines IL-10 to the donors reduces IRI and improves lung functions 12–24 hours before organ retrieval [46].

Finally, in the last few years, an increasing interest has been centered on the immunological mechanisms of sterile inflammation involved in IRI with the aim to find new strategies to modulate this process and reduce the inflammatory component associated with the activation of the immune system.

1.2 Sterile inflammation and danger theory

The cell death associated with the mechanisms of cellular damage previously described in IRI generates the condition for an inflammatory process. The rupture of plasma membranes associated with necrosis is, in fact, responsible for the release of intracellular contents which are typically "hidden" in quiescent states. These factors can activate immune responses and triggers an inflammatory reaction. However in this case, unlike the inflammatory conditions induced by pathogen infection, the entire complex of molecular and cellular events is entirely activated by endogenous products. For this reason, the acute inflammation triggered by IRI as well as by others chemical, mechanical and metabolic sources of injury is defined as "sterile inflammation."

Neutrophils are the most represented cellular subset acutely infiltrating the area of tissue injury and bacterial infection [47]. However, in the contest of sterile inflammation, neutrophils would not function as antimicrobial effectors, and their task would mainly consist in the removal of the cellular debris released by damaged cells. This scavenging function exerted by neutrophil represent a protective mechanism which allows the removal of potentially pro-inflammatory mediators and initiate the healing process of wounds [48]. In this setting, increasing evidence shows that neutrophils play a crucial role as

orchestrators in the resolution of tissue injury, contributing to limiting autoimmunity phenomena resulting from sterile inflammation [49]. However, an excessive or prolonged infiltration of neutrophils can exacerbate the initial tissue injury by aggravating the inflammatory environment. Activated neutrophils can promote tissue damage through increased oxidative stress, releasing cytotoxic mediators and recruiting other inflammatory cells. For this reason, neutrophil infiltration and activation have to be a very highly regulated process to maintain tissue hemostasis [47].

Although sterile inflammation is a well-known phenomenon, the precise mechanisms that regulate the activation of innate immunity to the self-antigen released with cell necrosis are not yet entirely clear. To explain this particular situation, not entirely justified by the classical self–non-self-theory, Matzinger suggested a rival theory, called the "danger theory" [50].

According to the danger theory, immune responses are not directly related to the presence of "nonself" (i.e., genetically foreign entities), but to the emission, within the organism, of "danger signals " or "alarm signals," released in response to damage [50]. This new paradigm also implies that self-constituents can trigger an immune response, if they are recognized as dangerous (i.e., cellular stress, some autografts); At the same time non-self elements can also be tolerated, if they are not considered dangerous (i.e., the fetus or commensal bacteria).

1.2.1 Damaged Associated Molecular Patterns and Pattern Recognize Receptors

Cell damage and necrotic cell death lead to the release of pro-inflammatory molecules named after DAMPs [51]. These molecules represent a sign of injury that can direct the immune system and stimulate sterile inflammatory responses. Research has recently focused on the characterization of these endogenous inflammatory signals and, as a consequence, the list of DAMPs that may trigger sterile inflammation is continually expanding.

At the current state, DAMPs are classified into two major categories:

(1) **Intracellular** substances passively released from necrotic cells or actively from stressed cells (including high mobility group box 1 (HMGB-1), ATP, monosodic urate, and others).

(2) **Extracellular** substances that become "active" in a pro-inflammatory state after tissue injury (including short hyaluronan fragment (HA), collagen-derived peptides and others)

The multitude of DAMPs released and generated at sites of sterile lesions produce a complex environment of inflammatory mediators that is detected by the innate immune system through the expression of specific receptors bearing to the large family of the Pattern Recognize Receptors (PRRs) [52]. Based on their localization on the cell surface or their presence in cytoplasmic compartment, PRRs can also be distinct in two major categories. Membrane-bound forms include Toll-like receptors (TLRs) and C-type lectin receptors. Nucleotide-binding oligomerization domains (NOD)-like receptors (NLRs) and RIG-I-like receptors (RLRs) are instead located in the cytoplasm [53].

The engagement of PRRs with DAMPs is critical for the recruitment and activation of the innate immunity in the site of tissue injury and represents the immunological link between tissue damage and sterile inflammation [54].

At the current state, several DAMPs and relatives PRRs have been demonstrated to play a role in IRI after solid organ transplantation. In this regard, HMGB1 is probably one of the best-characterized. HMGB1 is a nuclear protein that regulates gene transcription whose circulating levels have been demonstrated to be increased in several models of IRI [55-58]. HMGB1 levels have also been found increased in the damaged organs and its pharmacological blockade has proved to attenuate inflammation [59, 60]. In human lung recipients, high levels of extracellular ATP in the airway have been linked to PGD risk [61]. Depletion of extracellular ATP with recombinant apyrase in a dog model of warm lung ischemia-induced ALI and in a rat model of orthotopic LTx-mediated PGD attenuated pulmonary edema and improved pulmonary lung function [61, 62].

Hyaluronan, a glycosaminoglycan produced by mesenchymal cells has also been found increased in murine models of IRI [63]. In his quiescent, noninflammatory states, hyaluronan exists in a high molecular weight form, which undergoes degradation upon inflammation. After activation, HA can trigger TLR2 and TLR4 dependent inflammation [64]. Interestingly, in an orthotopic lung allograft model, HA was demonstrated to abrogated transplant tolerance contributing to inflammation and acute graft rejection [65].

In conclusion, DAMPs release and PRRs activation seem to be an ongoing mechanism playing a major role in the early event following solid organ transplantation [54]. DAMPs-PRRs axis seems to regulate the extension of the initial inflammatory reaction modulating the immune response to the allograft. However, despite the

information derived from some of these proinflammatory mediators such as HMGB1 or HA, very few it is known regarding the possible contribution of others DAMPs that have been described to play a role in different model of sterile inflammation. To this regard, increasing evidence *in vivo* and *in vitro* suggests that DAMPs derived from mitochondria contribute to sterile inflammation, promoting the activation and the recruitment of inflammatory cells to the area of tissue injury [66].

1.2.2 Mitochondrial DAMPs

The hypothesis that some organelles evolved from the symbiotic union of two different organisms dated the late nineteenth century and was firstly formulated by the botanist Andreas Schimper. Based on his observation on chloroplast division in green plants, he noticed that these organelles were very similar to free-living cyanobacteria. It was then Ivan Emanuel Wallin, in the early decades of the twentieth century, to formally propose a symbiogenesis theory which suggested that mitochondria originated from symbiotic bacteria. However, their ideas were largely ignored until the 1960s when the development of electron microscopes allows cellular ultrastructural study. Finally, in 1967, Lynn Margulis proposes what is now known as the endosymbiotic theory. According to the endosymbiotic theory, mitochondria evolved from ancient symbiotic prokaryotes that were absorbed into the ancestor of the eucaryotic cell **(Fig. 1.4)**. Consistent with this hypothesis is the evidence that mitochondria have their own DNA located inside the organelle in the form of circular chromosomes. Also, the mitochondrial genome (Mt-DNA) contains CpG unmethylated DNA repeats and codes for formylated peptide which are typical bacterial characteristics [67].

Along with their DNA and protein composition mitochondria share with bacteria their antigenic properties [68]. For this reason, the release of mitochondria in response to cell damage exposes CpG DNA repeats and formylated peptides to the innate immune cells that can detect those antigenic sequences trough specific PRRs. The role of Mt-DAMPs (Mt-DNA and Formylated peptides) in promoting systemic inflammation in response to trauma has been described in 2010 by Zhang et al. which firstly provided direct evidence suggesting that Mt-DAMPs represent one of the key mediators responsible for the link between injury and inflammation [69].

The CpG unmethylated DNA repeats of the Mt-DNA can be recognized by immune cells through the interaction with intracellular TLR9. As CpG DNA is internalized through endocytosis, TLR9 relocates to the endocytic vesicles. The co-localization of CpG DNA and TLR9 in the endosomes induces the recruitment of MyD88 to initiate an NFκB, p38 MAPK signaling [70]. The final effect of TLR9 signals is the activation of the immune cells and the release of proinflammatory cytokines such as type-I interferon, IL-6, TNFα, IFNα, and IL-12 [71].

In a mouse model of cardiac transplant, TLR9 activation prevented acceptance of fully allogeneic cardiac allografts suggesting a possible role for Mt-DNA in in the field of solid organ transplant [72]. Higher levels of circulating Mt-DNA have been measured in several inflammatory conditions associated to increased cell death such as trauma, sepsis and also coronary artery disease [73-75]. In a prospective observational cohort study of ICU patients, the analyses of Mt-DNA levels on blood samples reveal that higher levels were associated with increased mortality on ICU [76]. However, if Mt-DNA is released

early after LTx and whether their circulating levels may be associated with worst outcomes for these patients is yet not clear.

Mt-DNA codes for formylated mitochondrial proteins [77]. Protein synthesis is initiated with methionine or formylmethionine in all organisms studied to date [78]. In particular in eubacteria such as *Escherichia coli*, following aminoacylation of the initiator methionine tRNA ($tRNA^{fMet}$), the methionyl-tRNA ($Met\text{-}tRNA^{fMet}$) is formylated to formyl methionyl-tRNA ($fMet\text{-}tRNA^{fMet}$). As a consequence, protein synthesis in eubacteria is initiated with formylmethionine [78]. fMet-tRNA has also been discovered in eukaryotic organelles such as chloroplasts and in the mitochondria providing evidence that protein synthesis in mitochondria is initiated, as in eubacteria, with formylmethionine [79].

N-formyl peptides are cleavage products of mitochondrial proteins and, like their bacterial counterparts, are potent chemotactic factors for neutrophils *in vitro* and *in vivo* [69]. They activate a seven-transmembrane domain Gi protein-coupled receptors (GPCR) present on phagocytic cells named FPR1 and their binding causes calcium mobilization, activation of the NADPH oxidase, and degranulation [80].

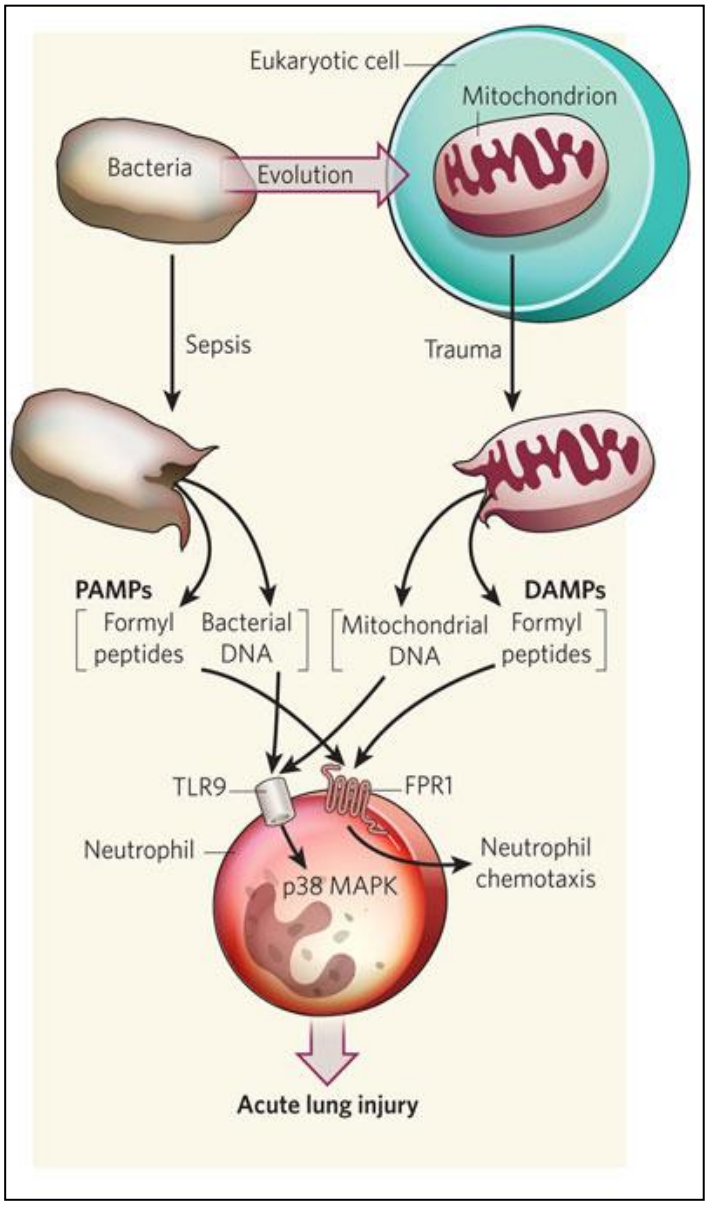

Fig. 1.4 The role of Mt-DAMPs in sterile inflammation

The Mt-DNA released by tissue injury can activate neutrophil TLR9 at the same extension of the bacterial DNA. TLR9 engagement induces p38 MAPK signaling leading to neutrophil activation. Similarly, formylated peptides released from bacteria and mitochondria activate the FPR1 and attract neutrophils promoting their chemotaxis to the sites of inflammation and injury [81].

1.2.3 Formyl peptide receptors

Bacterial and mitochondrial proteins are the only source of N-formyl peptides in nature and the consensus is that N-formyl peptide receptors have evolved to mediate phagocyte migration to sites of bacterial invasion and tissue injury [80].

The human FPR family includes the FPR1, FPR2/ALX (lipoxin receptor), and FPR3, which are well-conserved GPCRs involved in the initiation, propagation, and resolution of inflammation [82]. FPR1 was the first neutrophil GPCR to be cloned and sequenced. It is identified as a 350-residue seven-transmembrane receptor with the N-terminus and three loops exposed on the cell surface for ligand interactions and the C-terminus and the remaining loops in the cytoplasm necessary for intracellular signaling [83]. FPR1 has two separate but relatively conserved low-affinity homologous receptors, initially termed FPR-like 1 (FPRL1) and FPR-like 2 (FPR2L) which have been recently renamed FPR2/ALX and FPR3 [84]. All three receptors are clustered together on chromosome 19q13.3 and share significant sequence homology [85]. FPR1 synthesis occurs late in neutrophil maturation and is constitutively expressed on the surface of quiescent neutrophils. It is stored in the neutrophil primary granules and secretory vesicles and is rapidly up-regulated in response to a wide number of inflammatory stimuli [86]. Alongside FPR1 transport from intracellular compartments, neutrophil activation also increases FPR1 protein synthesis [87].

FPR1 signaling cascade consists of a highly complex and integrated chain of intracellular events which not only lead to the neutrophil cytoskeletal reorganization, critical to mediate cell adhesion, transmigration, and phagocytosis but also promote the NADPH dependent respiratory burst **(Fig. 1.5)**.

FPR1 has been described across several species, including rodents. In particular, the murine orthologue of human FPR1 share 77% of sequence homology, it is expressed at the same extension on similar cell types, and induce the same effects on neutrophil chemotaxis, degranulation, cytokine production, and phagocytosis [88].

Evidence show that FPR1 plays a critical role in mediate Mt-DAMPs proinflammatory effects mainly directing neutrophil migration to the area of necrosis. To this hand, Zhang et al. demonstrated that the *i.p*. injection of isolated Mt-DAMPs was sufficient to induce an FPR1-dependent peritoneal neutrophilia [69]. Moreover, when Mt-DAMPs were administered *i.v.*, alveolar neutrophil accumulation and pulmonary extravascular leak were observed in rats [66]. Also, using spinning-disk intravital microscopy in a mouse model of heat-induced focal sterile liver injury, McDonald et al. were able to demonstrate that an intravascular gradient of chemokines guides neutrophil migration along the vascular endothelium to regions of sterile inflammation. However, once in the extravascular space, neutrophils migrated toward the area of necrosis in an FPR1-dependent manner. In this study, $FPR1^{-/-}$ neutrophils exhibited a nondirectional migration within the tissue, and they failed to enter the necrotic area [89]. This motion behavior does not appear to be organ-specific as a similar hierarchy of chemotactic signals was observed within areas of sterile skin inflammation [90].

FPR1 has been proposed to be involved in some model of lung inflammation such as smoked induced emphysema [91] and acid aspiration related ARDS [92].

Moreover, a recent work by Honda et al. suggests that FPR1 may be involved in control the sterile inflammation associated with the warm IRI in liver [93]. However, what is the exact contribution of FPR1 in regulation neutrophil migration into the lung and whether

FPR1 may play a role in exacerbating the early graft injury associated to the LTx is currently not known.

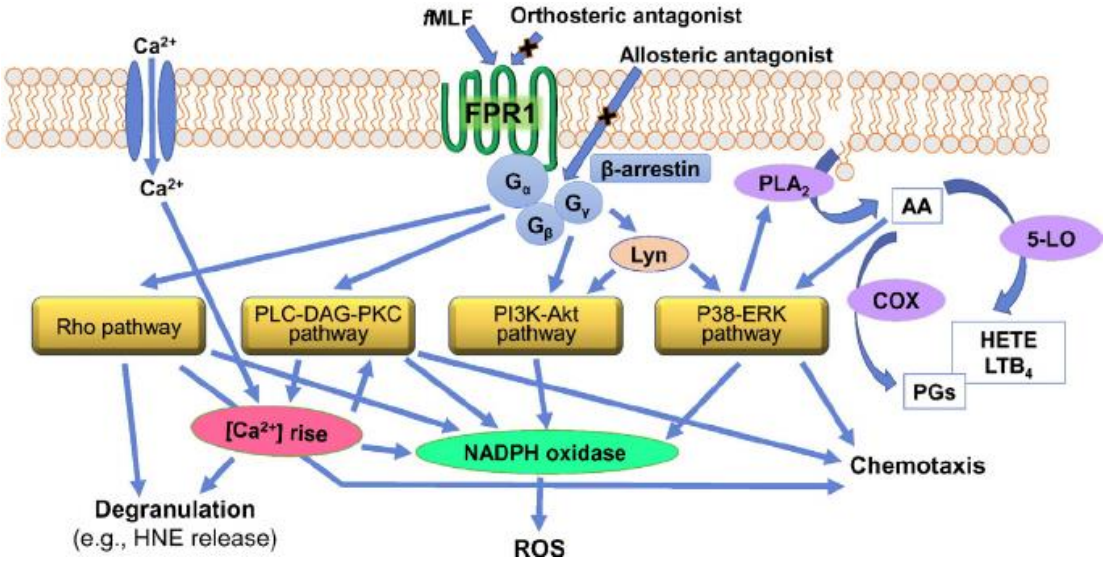

Fig. 1.5 Neutrophil FPR1 signaling

FPR1 activation regulates three main intracellular kinase pathways, including phosphatidylinositol-3-kinase (PI3K), protein kinase C (PKC), and mitogen-activated protein (MAP) kinases p38/extracellular signal related kinases 1 and 2 (ERK 1/2). In addition, PKC-independent pathways can be activated through the Src- related tyrosine kinase, Lyn. Rho GTPase pathways also play key roles in regulating a variety of neutrophil functional responses. PKC-independent pathways can be activated through the Src-related tyrosine kinase, Lyn. Activation of protein kinase C (PKC) and mitogen-activated protein kinase (MAPK) and elevation in intracellular Ca^{++} also results in the activation phospholipase A 2 (PLA2), leading to arachidonic acid (AA) release. AA is metabolized by 5-lipoxygenase (5-LO) and cyclooxygenase (COX), and products of this metabolism [hydroxyeicosatetraenoic acid (HETE), leukotriene B 4 (LTB4), prostaglandins (PGs), etc.] can act in an autocrine manner [94].

1.3 Neutrophils

At the end of the nineteenth century, Paul Ehrlich identified a new cell element which he defined neutrophil based on tinctorial properties and polymorphonuclear based on nuclear morphology. Subsequently, Il'jj Mečnikov, attributed to neutrophils a central role in immune responses through the discovery of the mechanism of phagocytosis.

The role of neutrophils in organ transplantation has been historically under-evaluated especially if compared to the high interest reserved to the adaptive immune cells. However, new insight into the mechanism of sterile inflammation not only revealed that neutrophils are usually the first leukocytes to infiltrate transplanted organs but also that they play a major role in exacerbating graft injury.

1.3.1 Neutrophils origin and maturation

Mature neutrophils account for about 50-70% of circulating leukocytes in humans. Their half-life within the blood stream is very short and consists of about 8 hours. Their diameter range around 7-10 μm, their nucleus is segmented, and their cytoplasm is enriched by granules and secretory vesicles [95]. Neutrophils are continuously generated in humans within the bone marrow from a myeloid precursor through a process defined granulopoiesis. During granulopoiesis, neutrophil maturation progresses from the myeloblast stage through promyelocyte, myelocyte, metamyelocyte, band and mature neutrophil stages, with each successive division resulting in a slightly smaller cell with more nuclear contraction and less cytoplasmic RNA [96]. The daily production of neutrophils can reach up to 2×10^{11} cells [97]. The highest stimulus for granulopoiesis is represented by the granulocyte colony-stimulating factor (G-CSF) which is produced in

response to increased levels of IL-17A [98]. Lymphocyte produces IL-17A under the control of IL-23 [99]. During inflammatory processes, there is an initial increase in neutrophils. Subsequently, these neutrophils go to apoptosis and are phagocytized by resident macrophages and dendritic cells. Removal of such apoptotic residues represents an inhibitory stimulus for the same macrophages and dendritic cells to produce IL-23, which down-regulate IL-17A expression and exerts an inhibitory effect on G-CSF production. This tight control on granulopoiesis plays a key role in the resolution of the inflammatory processes [100]. In a recent work by Kreisel et al., an extended graft cold ischemia has been associated to increased G-CSF–mediated granulopoiesis and neutrophil graft infiltration which prevented the immunosuppression mediated lung graft acceptance [101].

1.3.2 Neutrophil granules

During their differentiation, neutrophils begin to produce a series of granules where microbial and pro-inflammatory molecules are accumulated [97]. Neutrophil granules are classically divided into three types. Primary granules are structures of 0.3 μm in diameter and represent the larger-size granules. They are formed in the early stages of neutrophil maturation in the transition from myeloblast to pro-myelocyte and predominantly contain myeloperoxidase (MPO) which plays a central role in oxidative stress. Other molecules are the defenses, lysozyme, and a series of protein serine such as neutrophil elastase (NE), proteinase 3 (PR3) and cathepsin G (CG). The second type of specific or secondary granules have smaller dimensions, around 0.1 μm in diameter, and are produced later during the myelocyte transition. They are characterized by the presence of the lactoferrin

glycoprotein. They also contain a series of antimicrobial molecules such as NGAL, hCAP-18, and lysozyme. The third class of granules, so-called tertiary granules, have even smaller dimensions and are produced in the later phases of cellular differentiation of neutrophils. Tertiary granules contain only a few microbicidal molecules and represent a deposit for many proteinases such as gelatinase and leuco-lysine [102]. The fourth class of granular structures presents in neutrophils is named secretory vesicles. These, unlike other granules, are not produced by the Golgi complex but are formed by endocytosis in the most advanced stages of maturation of neutrophils. Plasma-derived proteins such as albumin mainly represent their content. Also, membranes of secretory vesicles represent an important reservoir of membrane-bound surface molecules that play a role in neutrophil migration and activation [103]. The neutrophilic degranulation triggered by an increase in intracellular Ca^{++} is a type of exocytosis where the controlled release of granule contents occurs in response to a stimulus. This process is divided into four phases. The first step is the actin cytoskeleton rearrangement and the microtubules assemblage to ensure recruitment of the granules towards the plasma membrane. Subsequently, the outer membrane of the granules goes to adhesion and subsequent fusion with the internal portion of the plasma membrane. The formation of a pore in the neo-generated melted membrane finally allows the expulsion of the material contained in the granules [104].

1.3.3 Phagocytosis

Phagocytosis is a selective process that requires energy and consists in the ability of a cell to ingest and destroy foreign materials. Neutrophils are defined as phagocytes because phagocytosis is their predominant feature. The first phase of the phagocytosis consists in recognizing the foreign particle. Recognition can be directed if mediated by a receptor. In this case, the receptors involved in the direct recognition belongs to the class of PRRs which are able to recognize either self-and non-self antigenic sequences such as those respectively derived from DAMPs and PAMPs. The recognition can also be indirect when is mediated by opsonization. In this case, the surface of the foreign particles is covered by recognition molecules that are called opsonins. The major opsonins are constituted by immunoglobulins G (IgG), which are recognized by receptors for the crystallizable portion (FcγR) present on the phagocytes and proteins derived from the activation of the complement cascade (C3b, C3bi, and C1q) that are bound by specific receptors (CR1, CR2, CR3). Following recognition, the uptake is mediated by contractile proteins of the cytoskeleton that allow the cell to wrap the bacterium with its cell membrane and include it in a neo-formed organelle surrounded by a membrane (phagosome). The maturation of the phagosome leads to its fusion with the cytoplasmic neutrophil granules loaded with cytosolic and antimicrobial molecules. At the same time, NADPH subunits assembled on the phagosome membrane and start to produce ROS. These two events contribute to create a highly hostile environment for the ingested particles [105].

1.3.4 NADPH e ROS generation

Phagocytosis activates in neutrophils a process called "respiratory burst." This is a type of non-mitochondrial respiration that leads to the formation of ROS. The NADPH oxidase expressed by phagocytes is a multi-enzymatic complex: 2 molecules of the complex, p22 phox (subunit α) and gp91phox (subunit β), are constitutively located on the membrane and contains two EME and FAD groups necessary for the electrons transport to the O_2 contained in the phagosome. Two other proteins of 47 and 67 kDa, are present exclusively in the cytoplasm; a third p40 phox protein present in the cytosol appears to be involved in the stabilization of p47/p67 phox complex in resting phagocytes. Following cell activation, secretory vesicles blend with the phagocyte plasma membrane and the NADPH enzyme complex assembled. The activation of NADPH oxidase leads to the formation of $O2^-$ superoxide anion which is subsequently transformed into hydrogen peroxide [106]. The MPO enzyme, contained within the primary granules, catalyzes the conversion of hydrogen peroxide into sodium hypochlorite, which results to be a highly toxic product. Hydrogen peroxide can also be converted to oxydrile •OH or degraded by catalase in water and oxygen [107]. The critical role of NADPH oxidase in bacterial killing is clearly demonstrated by the increased susceptibility to infections found in patients with chronic granulomatous disease (CGD) in which NADPH-oxidase-forming proteins are absent, reduced or functionally defective [108]. Unfortunately, during sterile inflammation, neutrophil`s ROS can be inappropriately excessive leading to increased level of oxidative stress and irreversible cell damage and death. In this regard, CGD patients who encode hypofunctional mutations in gp91phox or p47phox exhibit significant protection from transiently induced upper limb IRI [109]. Moreover, in canine heart and rat liver models of

IRI neutrophil NADPH oxidase-mediated ROS generation was the predominant contributor to tissue damage [110].

1.3.5 Neutrophil migration

The area interested by an inflammatory reaction is generally characterized by a micro-environment rich in signal molecules derived from the pathogen and the tissue injury. The endothelial cells can either directly sense these proinflammatory mediators or indirectly be activated by the resident leukocytes. Endothelial activation involves a series of vascular events such as vasodilation and alteration of capillary permeability. In addition, the activated endothelial cells can release cytokines and express surface adhesion molecules such as P-selectin and E-selectin. All of these factors contribute, in turn, to the recruitment of circulating leukocytes. In particular, neutrophils express on their cell surface glycosylated ligands such as P-selectin glycoprotein ligand 1 (PSGL1). The mutual recognition of these surface adhesion molecules allows the neutrophils to slow down their run within the blood circulation and promote the neutrophil ‘’rolling’’ over the surface of the vascular endothelium. Failure to express P-selectin or treatment with P-selectin neutralizing antibody has been demonstrated to attenuate early graft injury in a rat model of orthotopic left LTx [111].

Activate endothelium is coated with chemotactic molecules capable of directing the movement of neutrophils and inducing conformational changes in their surface integrins, increasing their affinity for the endothelial counterparts. Neutrophils express high levels of LFA1 integrins (also known as α1β2; CD11a complexed with CD18) and MAC1 (also known as αMβ2; CD11b- complexed with CD18). Conformational changes induced by cell

activation allow binding with surface endothelial molecules such as ICAM1 and ICAM2. LFA1 binding with ICAM1 mediate cell adhesion and arrest on the surface of the capillary which in turn is required for the subsequent transendothelial migration [112]. After an initial decrease in ICAM1 observed in the early phase after lung ischemia, a following potent ICAM1 upregulation occurs in the lung which coincides with the increase in late neutrophil infiltration and increased pulmonary edema. This biphasic change in ICAM1 expression is consistent with the late phase neutrophil contribution to IRI and supports the critical role played by ICAM1-LFA1 interaction in mediating the intravascular migration of activated neutrophils [113].

Although the mechanisms of neutrophil migration inside the vasculature are well characterized in their molecular details, very few it is known regarding what regulates the neutrophil migration through the vessel and their subsequent motion behavior into the extravascular space.

1.3.6 Neutrophil "swarming"

Because of technical limitations in the identification of neutrophils at single-cell resolution and the direct observation of their live dynamics, the information about how neutrophils coordinate their motion behavior in the extravascular space is currently limited. It is thought that neutrophils migrate through the interstitium at a typical average speed of ~10 μm per minute, with peak velocities reaching 30 μm per minute. Then, once at the focus of injury or infection, they slow down to initiate their effector functions, such as phagocytosis, ROS release and the formation of neutrophil extracellular traps [114]. However, recent evidence is providing new insight in this area suggesting that during

their extravascular migration neutrophils exhibit a highly coordinated form of chemotaxis which leads to the formation of cluster reminiscent of the swarming behavior of insects [115]. Specifically, cluster formation is regulated by a sequential cascade of events which include a scouting, an amplification and a stabilization phase **(Fig. 1.6)**. Initially, a small number of scout neutrophils which are close to the damage site migrate towards the focus through a GPCR dependent signaling and form an initial small cluster [116, 117]. During the second phase, named amplification, a larger number of additional neutrophils from the interstitial space are attracted [116, 117]. This phase has been demonstrated to be strictly regulated by neutrophil-produced leukotriene B4 (LTB4), which acts as a paracrine communication signal between neutrophils. Interestingly, previous *in vitro* data showed that LTB4 can sensitize neutrophils to other short-range chemoattractant such as the formylated peptides, thereby relaying information between individual cells over long distances [118]. During the final phase, cluster stabilization, neutrophils remodel the extracellular matrix, which results in the disappearance of collagen fibers from the cluster core. Integrins and GPCRs have been shown to mediate the migration and the retention of neutrophils in the collagen-free zone [119]. At this final stage of the cluster neutrophil recruitment is progressively reduced and monocytes start to appear at the edge of the cluster [115].

Currently, two main migratory patterns have been identified in neutrophil clusters. In stable clusters, neutrophils considerably decrease their motility and enter a state of migratory arrest, which is generally observed following tissue damage by physical trauma. Consequently, they form a seal around the site of damage in an attempt to scavenge necrotic debris [116]. Alternatively, sustained active migration of neutrophils within clusters results

in the 'swarming' behavior that is commonly seen in response to infection [117]. Neutrophil swarming is associated with the transient assembly and disassembly of these aggregates with a tendency for the larger cluster to be more stable and less dynamic compared to the smaller cluster. However, sustained migration can also be observed in stable clusters, suggesting that intermediate form of cluster dynamic may be observed [115].

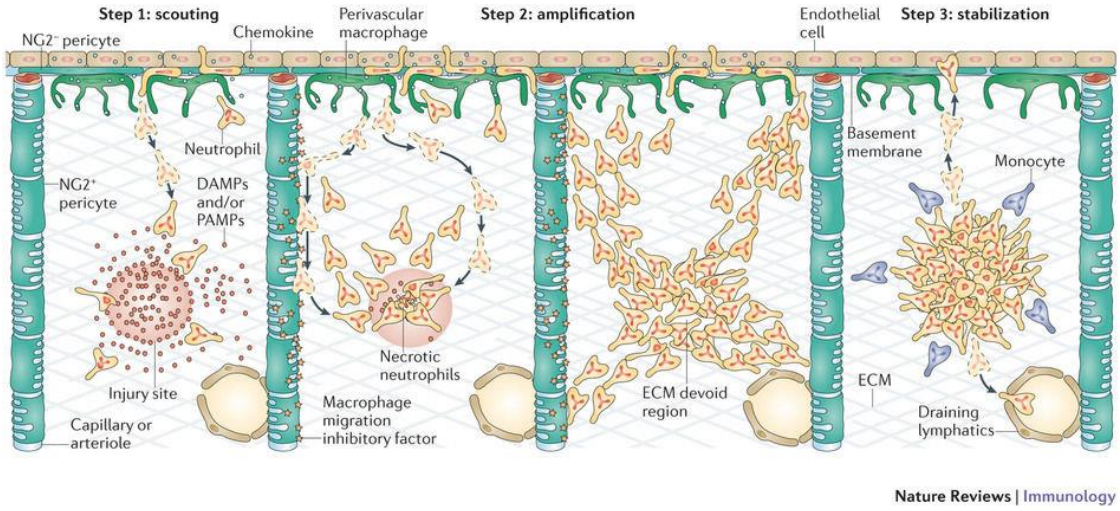

Fig. 1.6 Neutrophil migration in the extravascular space

Step 1: following an insult, 'scouting' neutrophils are attracted towards the injury site.
Step 2: activated 'scouts' amplify the response by producing leukotriene B4 (LTB4), which enables additional neutrophil recruitment from more distal regions.
Step 3: large numbers of neutrophils form stabilized clusters. At this stage, a further attraction of neutrophils ceases and Monocytes are present in the periphery of the clusters. Some neutrophils migrate away from clusters to the draining lymphatics, whereas others may also enter the vasculature and then travel to distant organs [114].

2. Aim of the study

LTx represents today a valid therapeutic option for end-stage pulmonary disease. In recent years there has been a significant increase in the number of LTx performed with progressive higher success rate mostly related to the improvements in organ selection and preservation, surgical techniques and effective immunosuppressive therapy. However, despite the improvements achieved, survival rates for LTx is still only about 50% to 5 years [120]. This is largely related to acute and chronic rejection, infectious complications and, in the early phase post-transplantation, to the IRI. The effects of IRI are responsible for a transplant-related form of ALI named PGD. PGD severity may range from a mild form of lung edema with no significant impairment of the respiratory function to a dramatic form of ARDS. The most severe forms of PGD, which account, according to the most recent statistics, for about 20-30% of the cases, are burdened by a high mortality rate and short and long-term complications ranging from a slow recovery of respiratory function to the development of chronic rejection [5, 11].

Increasing evidence suggest that higher DAMPs levels associated to tissue injury may play a critical role in exacerbating IRI through the intragraft recruitment and activation of immune cells [121]. Neutrophils represent the major component of the cellular network involved in the acute response to ischemia-reperfusion and their airways infiltration is considered a marker of tissue injury. Through the activation of PPRs expressed on their surface neutrophils can be specifically directed to the damaged area to scavenge cellular debris and initiate the resolution of the inflammatory process. Unfortunately, the response to a massive release of DAMPs, which may occur after trauma, surgery or IRI leads to an uncontrolled and aberrant infiltration of activated neutrophils which may be detrimental

exacerbating the initial injury. The role of Mt-DAMPs in promoting neutrophil activation and tissue damage has been recently described [69, 122]. However, whether Mt-DAMPs are released during LTx and if they may play a role in promoting PGD it still unknown.

The purpose of this thesis is to investigate the possible release of Mt-DAMPs after LTx and to evaluate how they may participate in the early immune response to the graft associated to the PGD. To this hand, we specifically explored the role of FPR1, a necrotactic receptor for Mt-DAMPs, in regulating intragraft leukocyte trafficking and ALI in the contest of LTx.

3. Matherials and Methods

Human Studies

All human studies were approved by the Washington University School of Medicine Institutional Review Board (#201012829). Serum and BAL were collected following written informed consent from all patients and healthy human volunteers.

Mt-DNA quantification

Peripheral whole blood was collected into EDTA-containing vacutainers (BD Sciences) within 6 to 12 hours upon arrival at the ICU. Samples were centrifuged at 2800 x g for 10 minutes and stored at -80°C until further analysis. Real-time PCR was performed in a BioRad CFX-Connect machine using 10 µl iQ SYBR Green Supermix (Bio-Rad), 0.5 µl of 5µM forward and reverse primers, 8.9 µl sterile water and 0.1 µl of cell-free plasma. Assays were performed in triplicate under the following conditions: 1 cycle at 95°C for 3 min, then up to 45 cycles at 95°C for 10 sec and 55°C for 30 sec and then a melt curve was performed from 65°C to 95 °C (0.5 °C every 5 sec). Primers for Human Mt-Cytochrome B (Mt-CytB; forward 5′-ATGACCCCAATACGCAAAAT-3′ and reverse 5′-CGAAGTTTCATCATGCGGAG-3′), Human Mt-cytochrome C oxidase subunit III (Mt-COXIII: forward 5′-ATGACCCACCAATCACATGC-3′ and reverse 5′-ATCACATGGCTAGGCCGGAG-3′) were synthesized by Invitrogen Custom DNA Oligos (ThermoFisher Scientific). Copy number was determined by comparison to a real-time PCR standard amplification curve generated from known amounts of purified Mt-Cytb and Mt-COXIII DNA amplified from the human PBMC of healthy control volunteers.

Mice

All studies were approved by the Washington University Animal Studies Committee. C57BL/6J (B6) and B6;129S-*Gt(ROSA)26Sor*$^{tm1(CAG\text{-}COX8A/Dendra2)Dcc}$/J (dendra2) mice were purchased from Jackson Laboratories (Bar Harbor, ME). LysM-eGFP on a B6 background were obtained from Klaus Ley (La Jolla Institute for Allergy and Immunology). FPR1$^{-/-}$ mice were purchased from Taconic Biosciences and maintained on a B6 background. FPR1$^{-/-}$ mice were intercrossed with LysM-GFP to obtain FPR1$^{-/-}$LysM-GFP mice. All mice used in these studies were of 6–9 weeks of age and maintained in a BSL2 facility.

Murine Lung transplantation

Animals weighing 22 to 28 grams were used as donors, and mice weighing 26 to 30 grams were used as recipients. Donor mice were anesthetized with an intraperitoneal injection of ketamine (50 mg/kg) and xylazine (10 mg/kg) before to be injected with 100 units of heparin into the penile vein. Mice were then euthanized with CO_2 5 minutes and the bodies were kept at room temperature for 90 minutes. After the foregoing warm ischemia experience, the donor chest was exposed through a median laparo-sternotomy and the left lung was removed, harvested in 4 ^{0}C LPDG preservation solution for 18 hours, and then orthotopically transplanted into the syngenic recipient mouse; donor/recipient pairs were chosen on the basis of designed experiments **(Fig. 3.1)**. Animals received humane care in compliance with the "Guide for the care and use of laboratory animals" prepared by the National Academy of Sciences and published by the National Institutes of Health and the "Principles of laboratory animal care" formulated by the National Society for

Medical Research. The whole surgical process was in accordance with the protocol of mouse left lung transplantation in our lab. [62, 123].

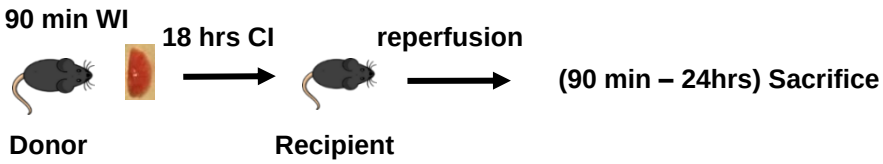

Fig. 3.1 Protocol of syngenic orthotopic left LTx

Early graft injury was obtained through a combination of warm and cold ischemia. The donor lung was exposed to 90 minutes of warm ischemia (WI) followed by 18 hours of cold ischemia (CI) in LDPG preservation solution. The injured graft was then transplanted into the syngeneic recipient and exposed to the reperfusion injury. The recipient was sacrificed at the indicated early (90 minutes) or late (24 hours) time points.

Mouse sample collection and processing

Mouse lung recipients were dissected under deep sevoflurane anesthesia at observation end-point (90 minutes or 24 hours after reperfusion) and required samples were collected. In order to collect BAL samples exclusively from the graft, the trachea was cannulated and the native lung was occluded trough hilar clamping. The left lung was then washed with 3 aliquots of sterile 0.1% FBS/PBS based buffer totaling 1 ml of final volume. The cellular component was separated from the BALf trough centrifugation at 500 xg. The first aliquot of the BALf was used for total protein and cytokines quantification. For serum sample, 0.5 ml of whole blood were collected by cardiac puncture in Microtainer SST tubes (BD Sciences) and centrifuged at 5000 xg for 20 minutes. Whole blood was alternatively collected in EDTA-containing vacutainers (BD Sciences) and lysed with ACK buffer

(Lonza) for the analysis of cellular components. The lungs were weighted and then minced with forceps in small pieces, suspended into a RPMI based digesting media containing Type II collagenase (0.5 mg/ml) (Worthing Biochemical Corporation) and 5 U/mL DNase (Sigma) and transferred to a 37°C incubator in mild agitation for 1 hour. The digested lung tissues were then passed through a 70-µm cell strainer in order to obtain a cell suspension. Spleen and both femurs and tibiae were also collected to respectively isolate splenocyte and bone marrow derived cells. Erythrocytes were lysed using ACK lysing buffer (Lonza).

Mitochondria analysis and purification

For both human and mice BALF was clarified of cells by centrifugation at 2800 xg for 10 minutes. The presence of cell-free mitochondria was assessed by using Mitotracker Green FM (Invitrogen), a probe that measures mitochondrial mass or by using transgenic mice which encode for specific mitochondrial dendra^{+} fluorescent protein. Mitochondria were fractionated from indicated tissues or BALF using a Mitochondria Isolation Kit (Miltenyi Biotec) with immunomagnetic beads specific for human or mouse TOM22 in accordance with manufacturer's recommendations.

Transmission Electron Microscopy

For ultrastructural analyses, isolated mitochondria from LTx recipient BALFs were fixed in 2% paraformaldehyde/2.5% glutaraldehyde (Polysciences Inc.) in 100 mM sodium cacodylate buffer, pH 7.2 for 1 hour at room temperature. Samples were washed in sodium cacodylate buffer and postfixed in 1% osmium tetroxide (Polysciences Inc.) for 1 hour. Samples were then rinsed extensively in dH20 prior to *en bloc* staining with 1% aqueous uranyl acetate (Ted Pella Inc.) for 1 hour. Following several rinses in dH20, samples were

dehydrated in a graded series of ethanol and embedded in Eponate 12 resin (Ted Pella Inc.). Sections of 95 nm were cut with a Leica Ultracut UCT ultramicrotome (Leica Microsystems Inc.), stained with uranyl acetate and lead citrate, and viewed on a JEOL 1200 EX transmission electron microscope (JEOL USA Inc.) equipped with an AMT 8 megapixel digital camera and AMT Image Capture Engine V602 software (Advanced Microscopy Techniques)

Lung graft injury

Lung weight was measured immediately after its excision (wet weight). The lung tissue was then dried in an oven at 60°C for 72 hours and re-weighed as dry weight. The W/D weight ratio was calculated by dividing the wet by the dry weight. BALF protein content was quantified by absorbance at 595 nm (μQuant-Biotek) using a Bradford kit Protein Assay (Bio-rad) and bovine serum albumin as a standard (BSA), (Sigma). For histology, the left lung grafts were harvested, inflation fixed in formaldehyde, embedded in paraffin, sectioned, and stained with hematoxylin and eosin.

Chemokine profiling by cytometric bead array

Detection of CXCL1, CXCL2, and CXCL5 from animal`s BALf was performed using ProcartaPlex Mouse Cytokine & Chemokine Immunoassays (eBioscience) according to the manufacturer`s instructions.

Flow cytometry analyses

Graft tissue, spleen and BAL were prepared as previously described. Cell pellets were resuspended in FACS buffer (PBS with 2% FBS and 0.4% EDTA) and Fc receptors were blocked with anti-mouse CD16/32 Abs (eBiosceince). Cells were stained with CD45 (eBioscience, 30-F11), CD11c (BD Pharmigen, HL3), Ly6C (Biolegend, HK1.4), Ly6G (Biolegend, 1A8), CD11b (eBioscince, M1/70). Cells absolute number was quantified by multiplying percentage abundance from the singlet cells gate by the total count of recovered cells. $CD45^+$ gate was used when the cell population was expressed as a percentage.

Neutrophil isolation and delivery into the airways

Neutrophils were purified by immunomagnetic bead-mediated negative selection with biotin-labeled Abs (eBioscience) specific for CD3e (145-2C11), CD4 (GK1.5), CD5 (53-7.3), CD8a (53-6.7), CD19 (MB19.1), B220 (RA3-6B2), CD49b (DX5), CD11c (N418), I-A/I-E (2G9), CD115 (AFS98), F4/80 (BM8), TER-119 (TER-119), CD117 (2B8). Labeled cells were fractionated with Streptavidin MicroBeads and LS MACS columns (Miltenyi Biotec). Isolated neutrophils ($5x10^6$/50µL) from LysM-GFP^+ and LysM-GFP^+ $FPR1^{-/-}$ mice were introduced into a B6 donor bronchus just before the transplant and the recipients were euthanized 90 minutes after reperfusion.

Intravital 2-Photon microscopy and data analysis.

Time-lapse imaging was performed with a custom-built 2Photon-microscope running ImageWarp acquisition software (A&B Software). Mice were anesthetized with an intraperitoneal injection of ketamine (50 mg/kg) and xylazine (10 mg/kg) and

maintained with halved doses administered every hour. Mice were intubated orotracheally with a 20-gauge angiocatheter and ventilated with room air at a rate of 120 breaths per minute and with a tidal volume of 0.5 ml. The left lung was exposed through a left thoracotomy, and the lung was imaged by using a custom-built chamber maintained at 37 °C. A small ring of VetBond was used to attach the lung tissue to the bottom of the cover glass without exerting pressure directly on the lung. 50 µl of Q-dot were injected from the penis vein in order to visualize the blood vessel. 2-Photon excitation produced a second harmonic signal from collagen around alveoli, thus providing a useful landmark for the air spaces. For time-lapse imaging of leukocyte migration in the tissue parenchyma, we averaged 15 video-rate frames (0.5 seconds per slice) during the acquisition to match the ventilator rate and minimize movement artifacts. Multidimensional rendering and manual cell tracking was performed with Imaris (Bitplane). Data were transferred and plotted in GraphPad Prism 6.0 (Sun Microsystems Inc.) for creation of the graphs.

Adhesion molecule expression

Bone marrow-derived neutrophils isolated as previously described from $FPR1^{-/-}$ and B6 mice were cultured at 37° C at the concentration of $1x10^6$ cells/ml in RPMI complete media. Mt-DAMPs, in the form of mitochondria isolated from lung homogenates, were used as a treatment and vehicle (saline) was used as a negative control. After 3 hours of incubation, cells were washed in cold FACS buffer and stained for surface antigen. The expression of CD11b on the $Ly6G^+$ $CD11c^-$ cells was calculated as Mean Intensity Fluorescent (MFI) by flow cytometry. For neutrophil cluster assay in vitro, isolated neutrophils were treated with Mt-DAMPs and cultured at 37°C for 1 hour in order to allow the formation of neutrophil cluster. Cultured cells were treated with an anti-CD11b

neutralizing antibody (10µg/ml) (BioXCell) or relative Isotype control (BioXCell) and viewed by optical microscopy at 200X magnification.

Statistical analysis

For human data, categorical variables were expressed as frequencies and percentages; continuous variables, by mean values and standard deviations. Differences between categorical variables were analyzed by Fisher exact test. The student's t-test (with Welch's correction when appropriate) was used to detect differences between continuous variables. The paired t test was applied to assess longitudinal differences in mean Mt-DNA levels between pre and post-transplant plasma samples. The Pearson product-moment correlation was computed to assess the relation between continuos variables and Mt-DNA levels. For mouse experiments, significant differences were evaluated with the non-parametric Mann-Whitney U test or with an unpaired Student t test if normally distributed. A one-way ANOVA or the equivalent non-parametric Kruskal-Wallis tests with post-hoc comparisons were used to analyze data with more than two groups. Statistical analyses were performed using GraphPad Prism 6.0 (GraphPad Software, Inc.) and a P value < 0.05 was considered significant.

4. Results

Mt-DAMPs are released into the airways of LTx

The increase in circulating Mt-DAMPs following trauma and surgery has been previously documented [122]. To determine if LTx-mediated IRI triggers the release of Mt-DAMPs into the injured airways, B6 mice received syngeneic lungs exposed to 90 minutes of warm ischemia and prolonged cold preservation. Analysis of the cell-free BALF one day after reperfusion using a fluorescent dye specific for mitochondrial mass show the increased of Mt-DAMPs when compared to sham-operated mice **(Fig. 4.1A)**. In addition, to discriminate among the recipient versus the donor source of Mt-DAMPs, we alternatively use donor lungs derived from transgenic mice expressing the fluorescent dendra2^{+} mitochondrial protein. The analysis of the cell-free BALF obtained one day after reperfusion reveals that the majority of the Mt-DAMPs found into the airways derived from the injured donor tissues **(Fig. 4.1B)**. Mitochondria were also directly isolated from BALf by positive selection and visualized by electron microscopy **(Fig. 4.1C)**. Consistent with the observation of increased Mt-DAMPs into the injured airways was the histological evidence of epithelial injury, leukocyte infiltration and luminal debris deposition in transplanted lung airways suggesting that Mt-DAMPs are released from necrotic cells **(Fig. 4.1D)**.

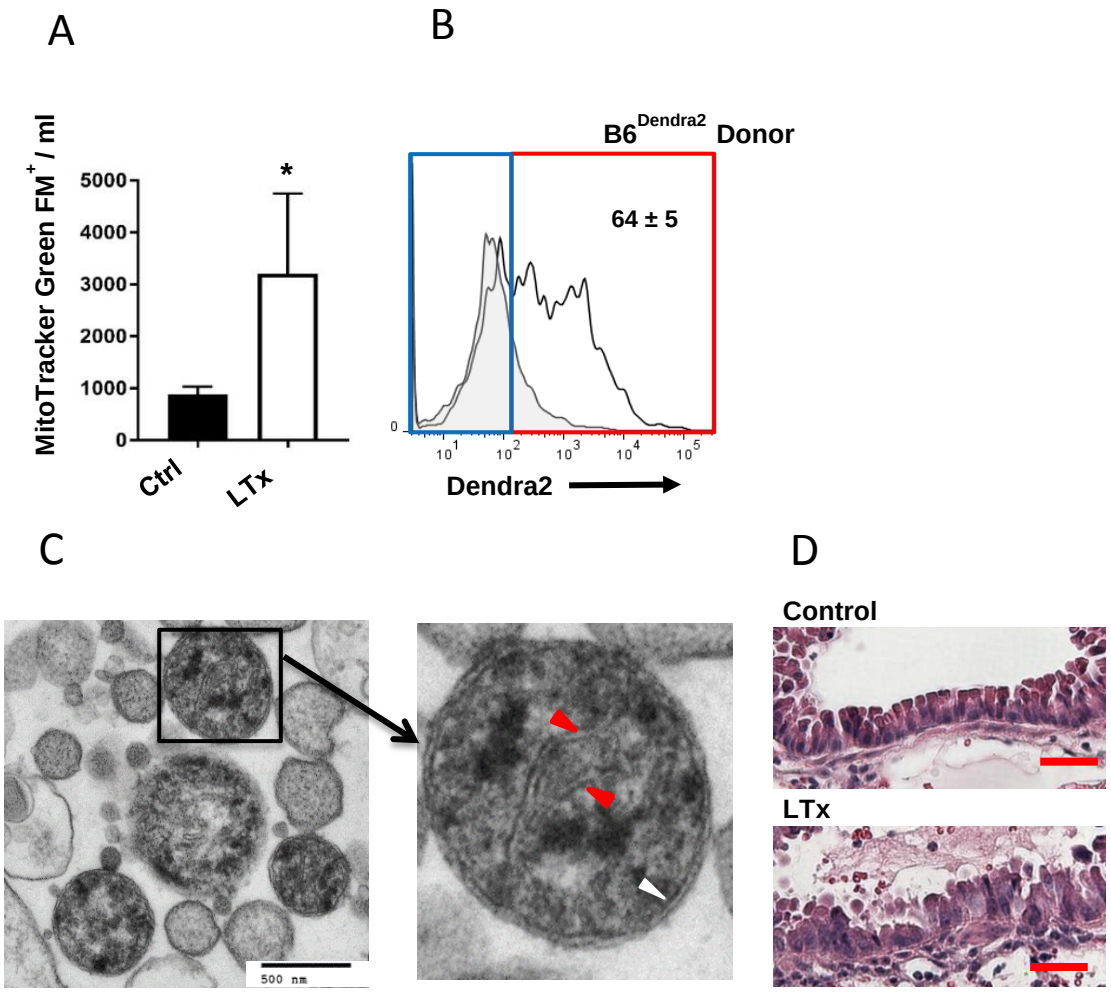

Fig. 4.1 Mitochondria release into the airways of LTxs

Mt-DAMPs from B6 → B6 recipient BALf or sham-operated B6 mice were stained with MitoTracker Green FM and counted by flow cytometry. **(A)** Histogram represents the mean number/ml of MitoTracker Green FM^+ events ± SEM where *p <0.05 (n = 5 / group). Mt-DAMPs were also isolated from the BALf of LTx recipients were Mito-$dendra2^+$ lungs were used as a donor. **(B)** Representative dot plot showing the percentage of donor ($dendra2^+$ in red) vs recipient ($dendra2^-$ in Blu) Mt-DAMPs (n = 5 / group). **(C)** A representative transmission electron micrograph (n = 3) of airway cell-free mitochondria where white and red arrows denote outer mitochondrial membrane and cristae, respectively. **(D)** Representative H&E histopathology of bronchiolar epithelium from a B6 → B6 lung graft (LTx) and the right un-transplanted lung (Ctrl) one day after reperfusion. Data are representative of at least five transplants (200X magnification, scale bar = 50 µm).

FPR1 expression in the recipient controls intragraft neutrophils distribution

Based on reports that show FPR1 promotes neutrophil trafficking towards gradients of Mt-DAMPs [69, 89, 122] we assessed intragraft neutrophil trafficking in FPR1 deficient mice. Transplant combinations were performed where either the donor or the recipient or both were deficient in FPR1. Histopathological analysis of lung grafts showed less intra-alveolar leukocyte infiltration in the $FPR1^{-/-}$ recipients irrespective of FPR1 expression in the donor graft **(Fig. 4.2A)**. Surprisingly, overall leukocyte infiltration in the lung appeared comparable in the different combination of LTx suggesting a role for FPR1 in regulating intragraft leukocyte distribution in different compartment of the transplanted lung. As neutrophils are the most predominant infiltrating leukocyte in acutely injured lungs we next assessed if FPR1 specifically regulated neutrophil recruitment to the lung grafts by separately analyzing BAL and graft tissue by flow cytometry **(Fig. 4.2B-C)**. As expected, despite a significant reduction in neutrophil BAL accumulation observed in the $FPR1^{-/-}$ recipients **(Fig. 4.2B)**, the overall neutrophil infiltration in non-airway tissues was not significantly altered between B6 and $FPR1^{-/-}$ recipients **(Fig. 4.2C)**.

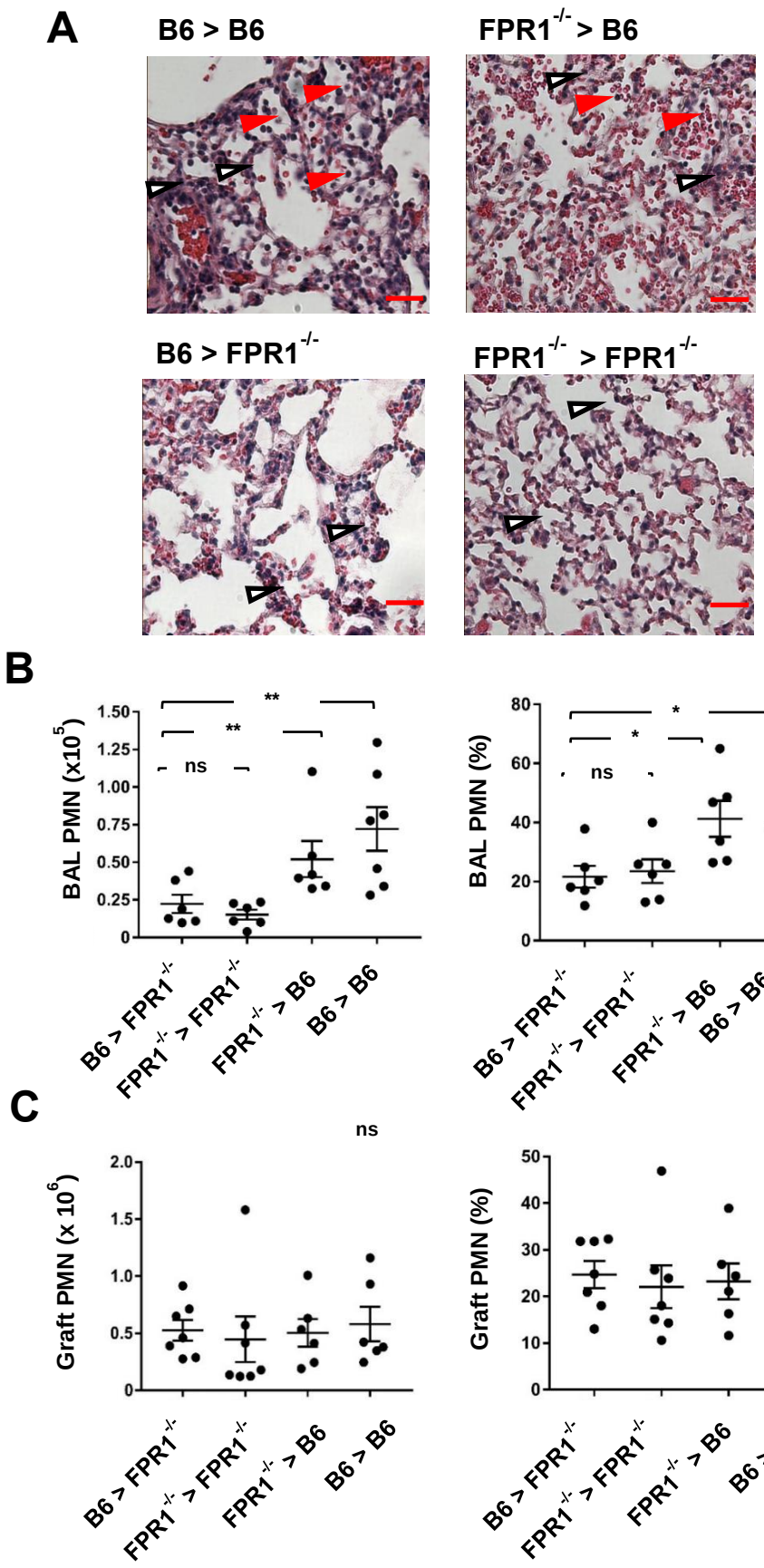
A
B6 > B6
FPR1-/- > B6
B6 > FPR1-/-
FPR1-/- > FPR1-/-
B
BAL PMN (x10^5)
BAL PMN (%)
ns
**
*
B6 > FPR1-/-
FPR1-/- > FPR1-/-
FPR1-/- > B6
B6 > B6
C
Graft PMN (x 10^6)
Graft PMN (%)
ns

Fig. 4.2 FPR1 expression in the recipient controls intragraft neutrophils distribution

(**A)** Lung grafts from indicated transplant combinations one day after reperfusion were assessed for polymorphonuclear infiltration within alveolar spaces (red arrowheads) and interstitium (white arrowheads) by H&E stain (200X, scale bar = 50μm, n = 3 / group). Neutrophil accumulation was also quantified as (left) total number and (right) percent abundance of the $CD45^+$ cells (mean ± SEM; *p<0.05, **p<0.01) in the BAL **(B)** compared to the total graft tissue **(C)**

Transendothelial migration and chemokine gradients are not altered in $FPR1^{-/-}$ recipients

Since neutrophil extravasation into the pulmonary interstitial spaces should precede trafficking into the airway we asked if FPR1 controls neutrophil transendothelial migration. Surprisingly, $FPR1^{-/-}$ neutrophils had comparable transendothelial migration rates relative to B6 neutrophils as evident by a similar ratio of intravascular and extravascular neutrophils in reperfused lung grafts **(Fig. 4.3A)**. Accordingly, we didn`t find significant differences in the numbers and percentage of B6 and $FPR1^{-/-}$ graft infiltrating monocytes, which has been previously reported to promote neutrophil extravasation into transplanted lungs [124] **(Fig**. **4.3B)**. Moreover, the BAL levels of the major chemokines involved in neutrophil migration were comparable in the B6 and $FPR1^{-/-}$ recipient indicating that the different intragraft distribution observed was unrelated to a different pattern of chemokine gradient **(Fig. 4.3C)**. Altogether, these data suggest that $FPR1^{-/-}$ control neutrophil intragraft trafficking mainly in the extravascular space and independently from a chemokine gradient.

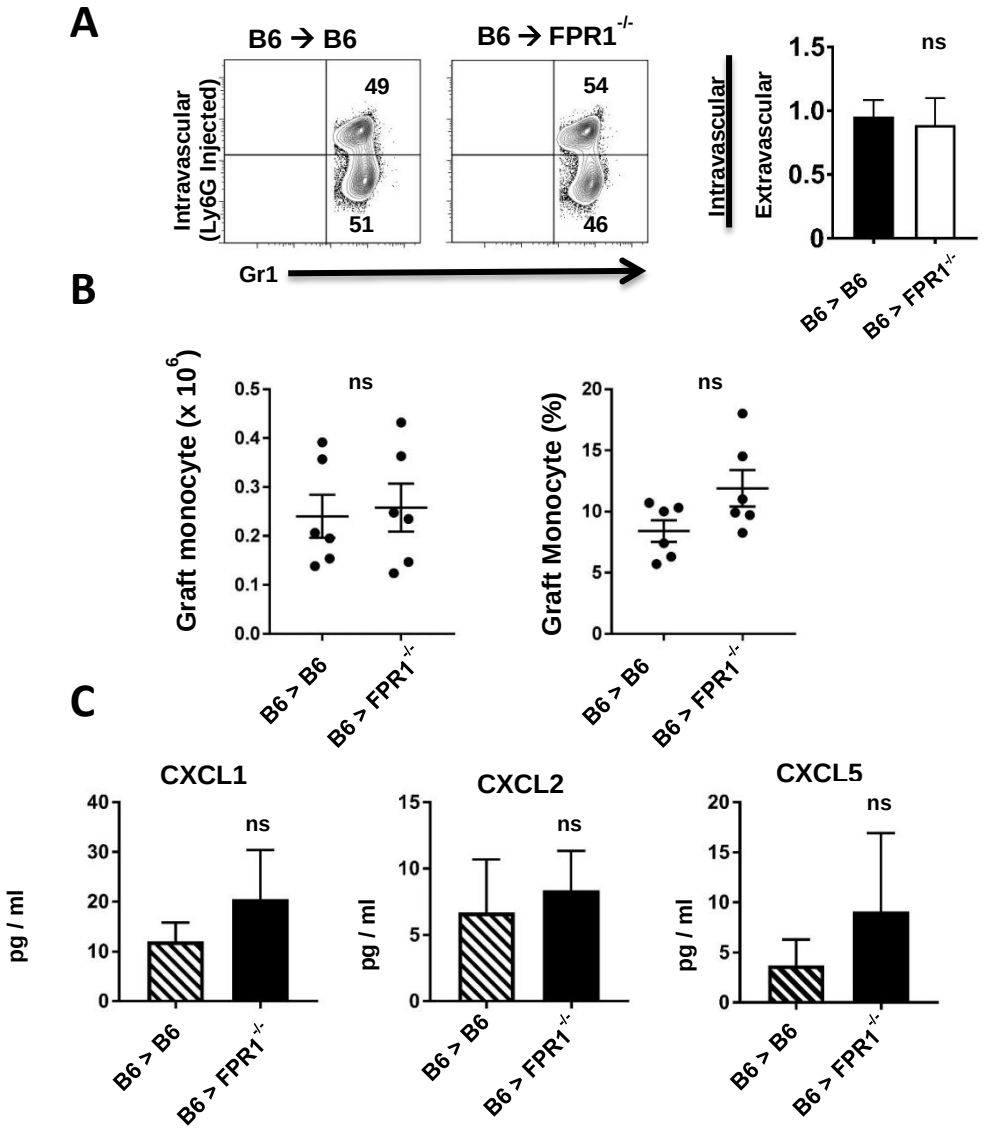

Fig. 4.3 FPR1 doesn`t control neutrophil transendothelial migration

B6 → B6 and B6 → FPR1$^{-/-}$ recipients were analyzed for neutrophil transendothelial migration. **(A)** Results are illustrated as (left) representative plots of the percent abundance of graft intravascular and extravascular neutrophils and (right) as a histogram showing the ratio of graft intravascular to extravascular neutrophils (n ≥ 3 / group; mean ratio ± SEM, n.s.) **(B)** Monocyte intragraft accumulation was also quantified as (left) total number and (right) percent abundance of the CD45^{+} cells (mean ± SEM). **(C)** Histogram showing B6 → B6 and B6 → FPR1$^{-/-}$ recipient BALF ELISA of CXCL1, CXCL2 and CXCL5 one day after transplant (n = 5 / group; mean ± SEM, n.s.).

Mt-DAMPs-FPR1 axis control neutrophil cluster stability and exit from airways

Since our data suggested that FPR1 contributes to airways neutrophilia regulating neutrophil dynamics beyond the vasculature we then investigated extravascular neutrophil trafficking behavior in lung grafts using intravital 2-photon microscopy. Both B6 and FPR1$^{-/-}$ neutrophils were typically mobile and predominantly observed aggregated within dynamic clusters **(Fig. 4.4A)**. However, neutrophil cluster stability was significantly attenuated in the FPR1$^{-/-}$ when compared to the B6. **(Fig. 4.4B)**. In order to understand if FPR1 regulates cluster stability in response to Mt-DAMPs exposure, we treated isolated neutrophils from B6 and FPR1$^{-/-}$ mice with Mt-DAMPs and we observed cluster dynamics *in vitro*. Our results not only show that Mt-DAMPs are sufficient to induce neutrophil clustering but also that, once clusters are formed, FPR1 expression contributes to their stability, as demonstrated by the reduced cluster area observed in the FPR1$^{-/-}$ neutrophils **(Fig. 4.4C)**. Recent findings suggest that neutrophil cluster in the site of injury requires the expression of adhesion molecules such as CD11b [90]. Accordingly, we found that the CD11b neutralizing Ab strongly reduced cluster stability either in the B6 and in the FPR1$^{-/-}$ neutrophils treated with Mt-DAMPs **(Fig. 4.4C)**. To prove that Mt-DAMPs-FPR1 axis regulates neutrophils CD11b expression we treated isolated neutrophils with Mt-DAMPs and we assessed by flow cytometry the levels of CD11b expression in the FPR1$^{-/-}$ compared to the B6 neutrophils. Interestingly, we found that Mt-DAMPs significantly increase neutrophil CD11b expression and that this effect is reduced in the FPR1$^{-/-}$ compared to the B6 neutrophils **(Fig. 4.4D)**. Consistently with the attenuated neutrophil CD11b upregulation observed in the FPR1$^{-/-}$ compared to the B6 in response Mt-DAMPs, we

noticed that the neutrophil average speed within clusters *in vivo* was significantly higher in the FPR1$^{-/-}$ compared to the B6 **(Fig. 4.4E)**.

The reduced neutrophil extravascular cluster stability associated with the higher speed observed in FPR1$^{-/-}$ compared to the B6 led us to hypothesize that FPR1 may contribute to airway neutrophilia by slowing the egress from this compartment and promoting neutrophil retention into the injured airways. To answer this question we introduced EGFP transgene expressing FPR1$^{-/-}$ and B6 neutrophils into the bronchi of B6 lung grafts injured by prolonged cold preservation. Following reperfusion, we tracked their exit from the airways through measuring their abundance in the BAL and in the remaining graft tissues. When compared to B6, more FPR1$^{-/-}$ neutrophils exited airway and entered the graft tissues **(Fig. 4.5A)**. In contrast, FPR1$^{-/-}$ and B6 neutrophils were nearly undetectable in the peripheral blood and spleen suggesting that they had not exited graft tissues **(Fig. 4.5B)**.

Collectively, we show that FPR1$^{-/-}$ mice exhibit a peculiar intragraft trafficking into the transplanted lung which is characterized by an overall increase mobility associated with a reduced expression of adhesion molecules, reduced extravascular cluster stability and reduced retention into the injured airways. Those characteristics are compatible with the different intragraft distribution initially described in the FPR1$^{-/-}$ compared to the B6 recipients and appear to be related to the recognition of Mt-DAMPs released into the injured airways after LTx.

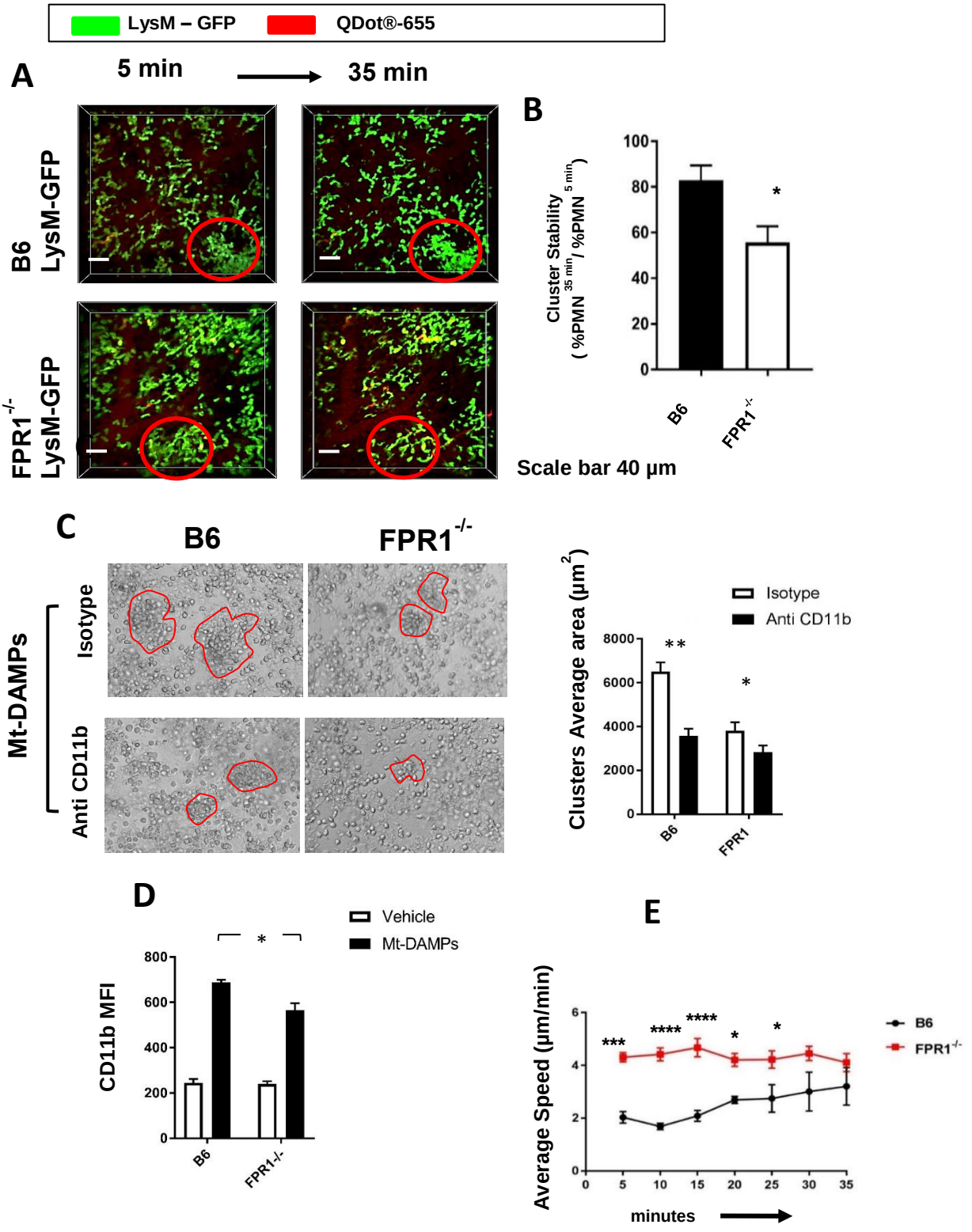
LysM – GFP
QDot®-655
A
5 min
35 min
B6 LysM-GFP
FPR1-/- LysM-GFP
B
Cluster Stability
(%PMN 35 min / %PMN 5 min)
100
80
60
40
20
0
*
B6
FPR1-/-
Scale bar 40 µm
C
B6
FPR1-/-
Mt-DAMPs
Isotype
Anti CD11b
Clusters Average area (µm2)
Isotype
Anti CD11b
8000
6000
4000
2000
0
**
*
B6
FPR1
D
Vehicle
Mt-DAMPs
CD11b MFI
800
600
400
200
0
*
B6
FPR1-/-
E
Average Speed (µm/min)
6
4
2
0
***
****
****
*
*
0
5
10
15
20
25
30
35
minutes
B6
FPR1-/-

Fig. 4.4 FPR1 slows neutrophil speed and increases cluster stability

B6 → LysM-EGFP B6 and B6 → LysM-EGFP FPR1$^{-/-}$ lung grafts were dynamically imaged by (**A**) intravital 2P microscopy 90 minutes after reperfusion (Neutrophil in Green and Vasculature in Red). Red circles show typical clusters **(**Scale bars = 40 µm). (**B**) Cluster stability was here defined as the ratio of the number of neutrophils within a cluster at the end of 30 minute imaging period to the number of neutrophils within the same cluster at the start of the 30-min interval period (mean ratio ± SEM; *p<0.05). **(C)**.Neutrophil cluster in response to Mt-DAMPs obtained from lung homogenates were also imaged *in vitro* by optical microscopy (6 random field/200X original magnification) in the B6 compared to FPR1$^{-/-}$ isolated neutrophils. Anti CD11b antibody (10µg/ml) or isotype control were used to test CD11b contribution to cluster stability. Clusters contour is emphasized by red lines. The bar graph shows neutrophil cluster stability here expressed as average area (µm^2) of the total number of clusters observed (n =3 / group; ** p<0.01,* p<0.05,). CD11b levels of B6 and FPR1$^{-/-}$ isolated neutrophils treated with Mt-DAMPs were measured by flow cytometry. **(D)** Bar graph showing the expression of CD11b quantified by MFI in the B6 compared to the FPR1$^{-/-}$ with and without Mt-DAMPs stimulation. **(E)** Individual neutrophils inside clusters were tracked for average speed (µm/min) over 5-min intervals up to a 30 min period. (mean speed ± SEM; ****p<0.0001, *p<0.001, ***p<0.05).

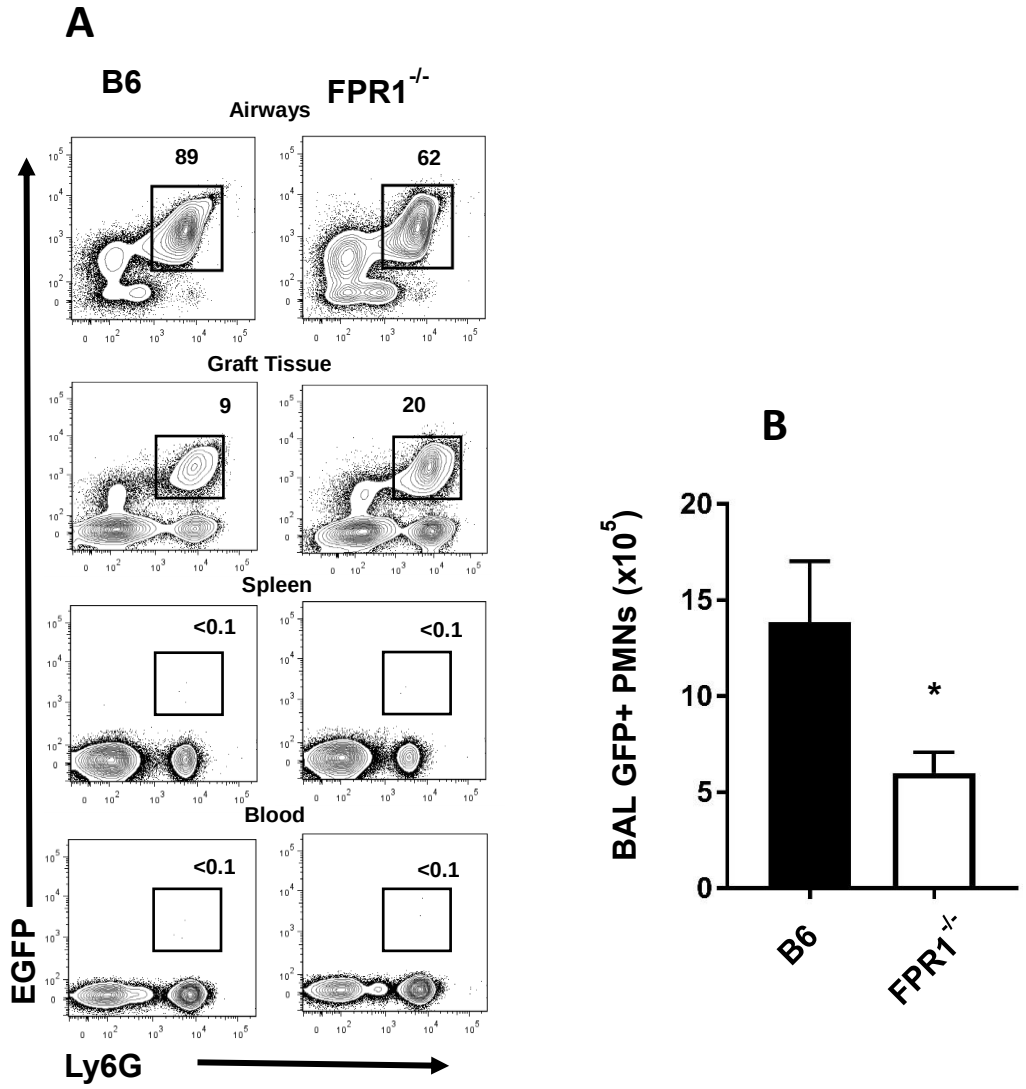

Fig. 4.5 FPR1 inhibits neutrophil egress from lung graft airways

Neutrophils ($1x10^5$/µL) isolated from B6 LysM-EGFP and $FPR1^{-/-}$ LysM-EGFP mice were introduced into the left main bronchus of B6 donor lungs that have undergone prolonged cold preservation and immediately transplanted into B6 recipients. Lung recipients were euthanized 90 minutes after reperfusion and $EGFP^+$ neutrophil distribution was tracked in the airway (BAL), in the graft tissues and in the periphery (spleen and whole blood) by flow cytometry. **(A)** Representative dot plots of $EGFP^+$ neutrophil percent abundance in indicated samples from 5 independent experiments. **(B)** Histogram shows mean number of $EGFP^+$ neutrophils retained in the airways (recovered from the BAL) (n =5 / group; * $p<0.05$,)

FPR1 expression in the recipient controls acute lung transplant injury

In order to understand if the different neutrophil behavior observed in the $FPR1^{-/-}$ neutrophils may be related to the development of the lung graft dysfunction, we assessed LTx injury in FPR1 deficient mice. Transplant combinations were performed where either the donor or recipient or both were deficient in FPR1. Histopathological analysis of lung grafts showed less diffuse alveolar damage in $FPR1^{-/-}$ recipients irrespective of FPR1 expression in the donor graft **(Fig. 4.6A)**. Additionally, lung graft edema and permeability were significantly reduced in B6 → $FPR1^{-/-}$ and $FPR1^{-/-}$ → $FPR1^{-/-}$ recipients relative to $FPR1^{-/-}$ → B6 or B6 → B6 recipients demonstrating that FPR1 on graft-infiltrating cells is sufficient to promote graft tissue damage **(Fig. 4.6B -C)**.

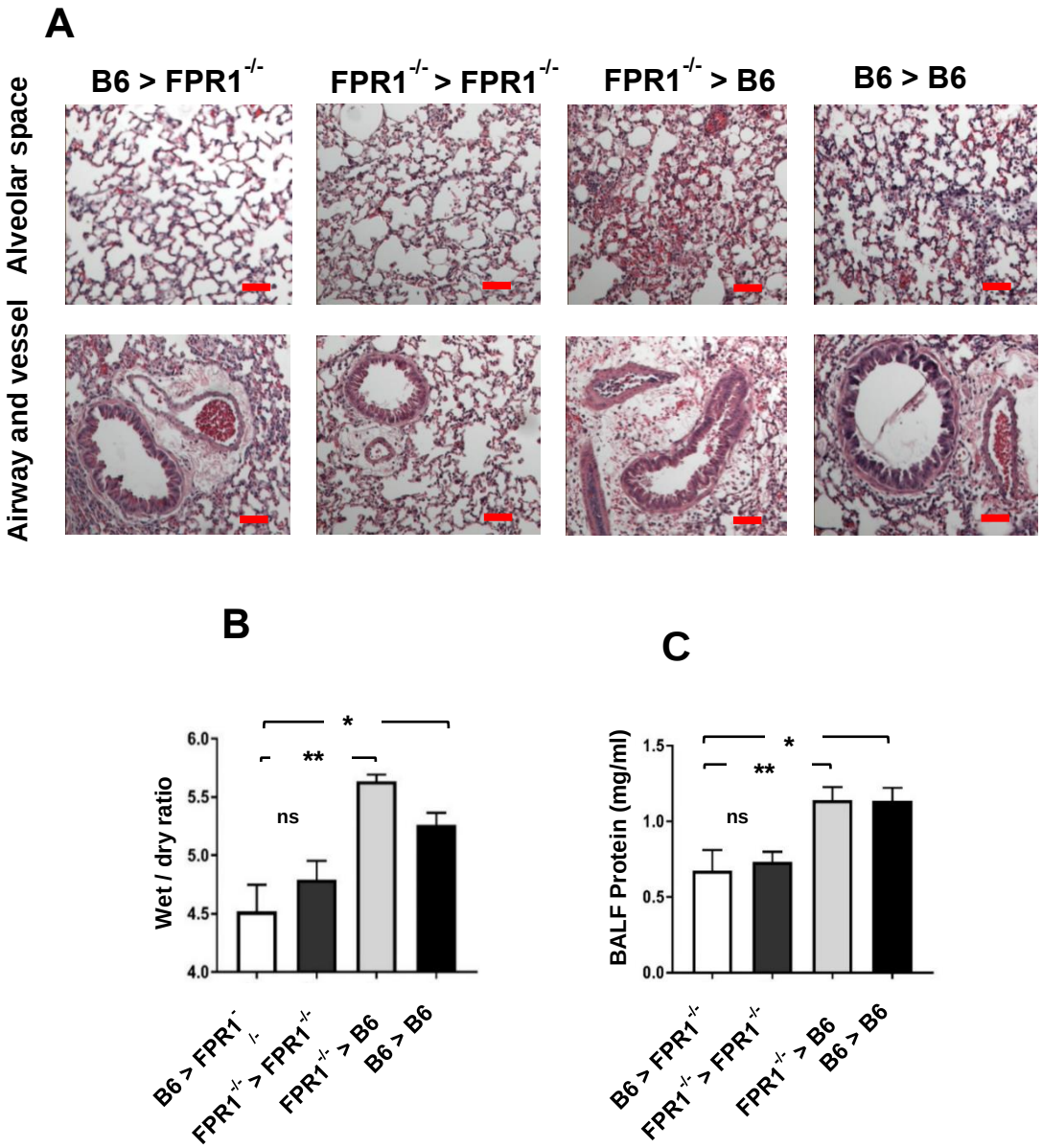

Fig. 4.6 Recipient FPR1 expression is sufficient to promote lung transplant injury. Indicated transplant combinations one day after reperfusion were analyzed for graft **(A)** H&E histopathology (100X, scale bar 200 µm (n= 3 / group), **(B)** edema by wet / dry ratio (mean ± SEM, n = 6 / group) and **(C)** BALF protein content (mean ± SEM, n = 6 / group). Where indicated *p<0.05 and **p<0.01.

Circulating Mt-DNA levels are elevated in lung recipients with PGD

To determine the clinical relevance of Mt-DAMPs release in human LTx we developed an *in situ* PCR-based quantitative method to measure the amount of mitochondrial cytochrome b (Mt-CYTB) DNA within the circulating plasma of 62 lung recipients and 10 healthy control volunteers. The clinical characteristics of the study participants are shown in **Table 4.1**. Circulating Mt-CYTB levels were nearly undetectable in healthy controls and slightly elevated in patients just prior to LTx. However, Mt-CYTB DNA levels rose significantly in lung recipient plasma obtained within 6 to 12 hours after arrival in the ICU **(Fig. 4.7A–B)**. Notably, post-transplant increases in Mt-CYTB DNA were not linked to disease indication, sex, donor age, body mass index, time of ischemia, or the use of cardiopulmonary bypass **(Supp. Fig. 4.1)**. Moreover, we also observed a comparable pattern of mitochondrial cytochrome III oxidase (Mt-COX III) DNA **(Supp. Fig. 4.2A-B)**.

We next asked if patients with severe PGD have a higher level of circulating Mt-DAMPs in the form of Mt-DNA. Patients with moderate to severe PGD at 24 and 72 hours post-transplant had significantly more circulating Mt-CYTB DNA when compared to patients with mild to no PGD **(Fig. 4.7C)**. Interestingly, most moderate to severe PGD sufferers with the highest accumulation of Mt-CYTB DNA early post-transplant continued to persistently manifest worst PGD score at 72 hours post-transplant **(Fig. 4.7D)**. Additionally, we observed a similar trend for Mt-COX III DNA levels for moderate to severe PGD patients at 72 hours post-transplant **(Supp. Fig. 4.2C-D)**.

	Total *n* 62	Time 0			Time 72 hrs		
		PGD 0-1 *n* 31 (50%)	PGD 2-3 *n 31* (50%)	p-value	PGD 0-1 *n* 53 (85.4%)	PGD 2-3 n 9 (14.5%)	p- value
Donor variables							
Age, (years)*	31 [21-49.5]	30 [20-49]	34 [21-51]	0.6	29.5 [20.5-48]	47 [28-58.5]	0.06
Female, n (%) †	28 (45.1%)	18 (58%)	10 (32.2%)	0.07	25 (47.1%)	3 (33.3%)	0.4
Recipient variables							
Age (years)*	61 [51-65]	61 [51-64]	61 [51-65]	0.5	61 [51-64.5]	64 [56.5-67.5]	0.1
Female, n (%) †	21 (33.8%)	8 (25.8%)	13 (41.9%)	0.2	15 (28.3%)	6 (66.6%)	0.05
Afro-American, n (%)†	5 (8%)	2 (6.4%)	3 (9.6%)	0.4	2 (3.7%)	3 (33.3)	0.0004
Body Mass Index (kg/m²)**	24.7 ± 4	23.6 ± 4.2	25.8 ± 3.5	0.03	24.6 ± 3.9	25.2 ± 4.6	0.6
Diagnosis:							
COPD, n (%) †	18 (29.1%)	11 (35.4%)	7 (22.5%)	0.4	15 (28.3%)	3 (33.3%)	0.7
IPF, n (%) †	26 (41.9%)	11(35.4%)	15 (48.3%)	0.4	22 (41.5%)	4 (44.4%)	0.9
CF, n (%) †	7 (11.3%)	4 (12.9%)	3 (9.6%)	0.9	7 (13.2%)	0	0.5
Others, n (%) †	11 (17.7%)	5 (16.1%)	6 (19.3%)	0.9	9 (16.9)%	2 (22.2%)	0.6
Surgical variables:							
Cardio Pulmonary Bypass n (%) †	21	6 (19.3%)	15 (48.3%)	0.03	16 (30.1%)	5 (55.5%)	0.2
Total preservation time (min) *	351 [285-510]	330 [283.8-403.5]	392 [290.5-527.5]	0.1	341 [284.5-464.8]	376 [323-585]	0.1

* Mann-Whitney U test. Values presented as median and interquartile range

** Unpaired T test. Values presented as mean ± SD

† Fisher exact test. Values presented as number and % of the column total

‡ Chi square test. Values are presented as number and % of the column total

Table 4.1 Patient's demographic and clinical characteristics

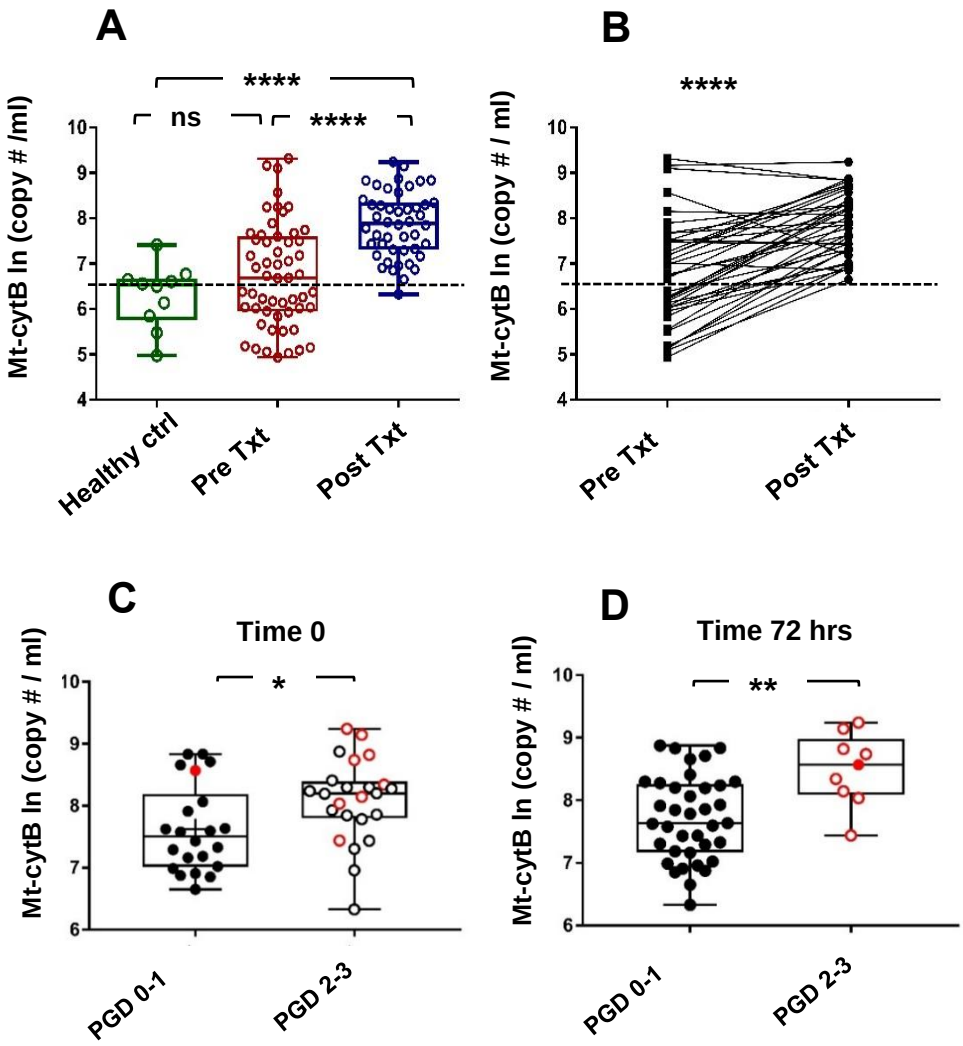

Figure 4.7 Human lung recipients with PGD have elevated circulating Mt-DNA
(A) Box and whiskers plot of circulating Mt-CYTB DNA levels obtained from lung recipients before LTx and within 6 to 12 hours after ICU arrival. (****p< 0.0001). **(B)** Paired analysis plot of Mt-CYTB DNA levels for each patient before and after LTx (****p<0.0001). The dashed line represents the threshold limit for Mt-DNA detection (background). Box and whiskers plot of circulating Mt-CYTB DNA levels measured in lung recipients with PGD 0-1 or PGD 2-3 graded at (**C**) time 0 (upon arrival at the ICU) and (**D**) 72 hours after ICU arrival (*p<0.05, **p< 0.01). Open red circles are patients who persisted with PGD 2-3 from time 0 to 72 hrs. The filled red dot represents a patient whose PGD worsened from PGD 1 at time 0 to PGD 3 at 72 hours.

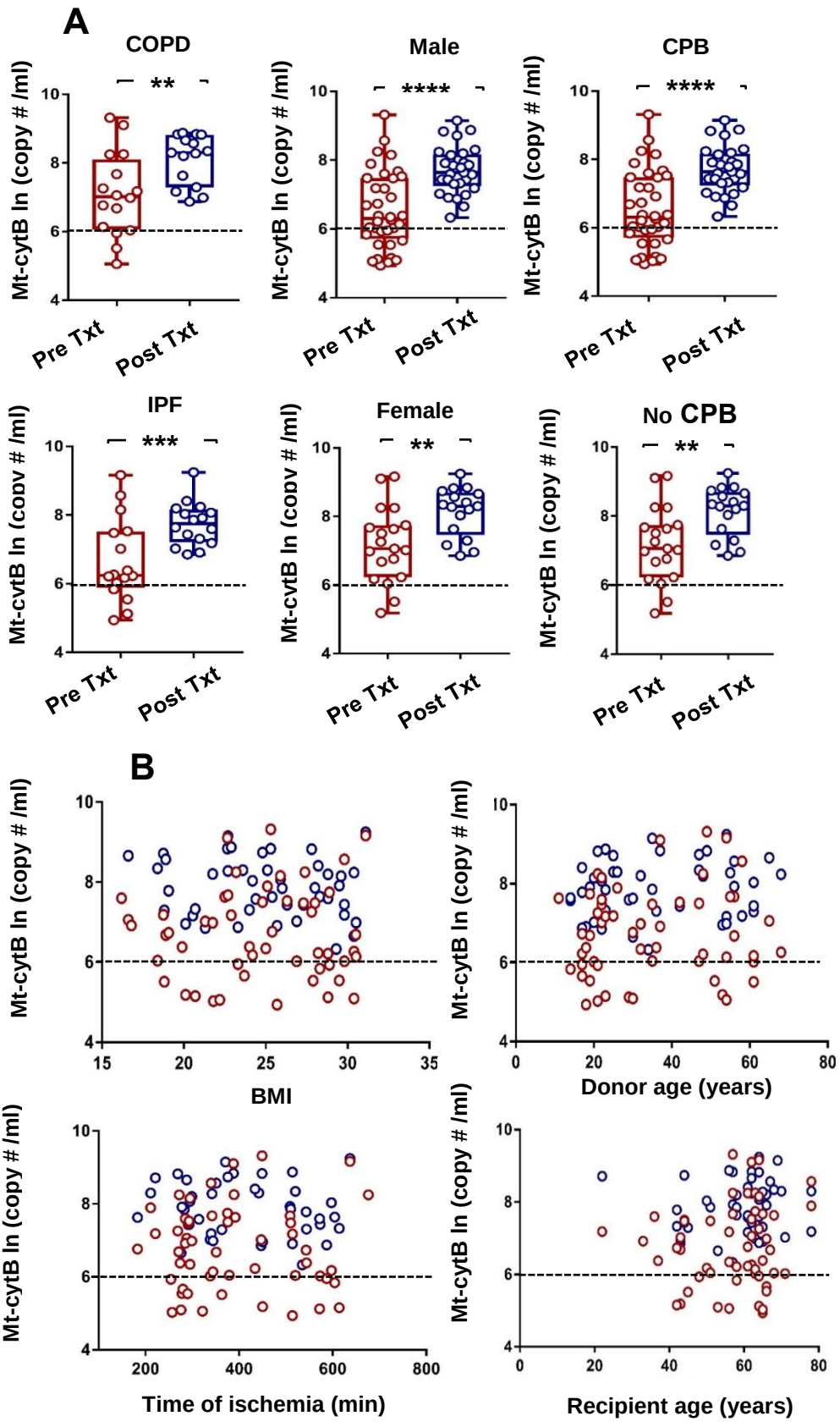
A
COPD
**
Male
****
CPB
****
IPF
***
Female
**
No CPB
**
Mt-cytB ln (copy # /ml)
Pre Txt
Post Txt
B
BMI
Donor age (years)
Time of ischemia (min)
Recipient age (years)

Supp. Fig. 4.1 Mt-DNA increase after LTx is independent from patient's characteristics

(A) Box and whiskers plot of circulating Mt-CYTB DNA levels obtained from lung recipients before LTx and within 6 to 12 hours after ICU arrival according to qualitative variable such as indication, gender and use of CPB. **(B)** Scatter plot of circulating Mt-CYTB DNA levels measured in lung recipients before LTx and within 6 to 12 hours after ICU arrival according to quantitative variables such as BMI, donor and recipient age and ischemic time. Dashed line represents the threshold limit for Mt-DNA detection (background). Red circle for pre-LTx and blue circle for post-LTx. (**p<0.01, *** p<0.001, ****p< 0.0001)

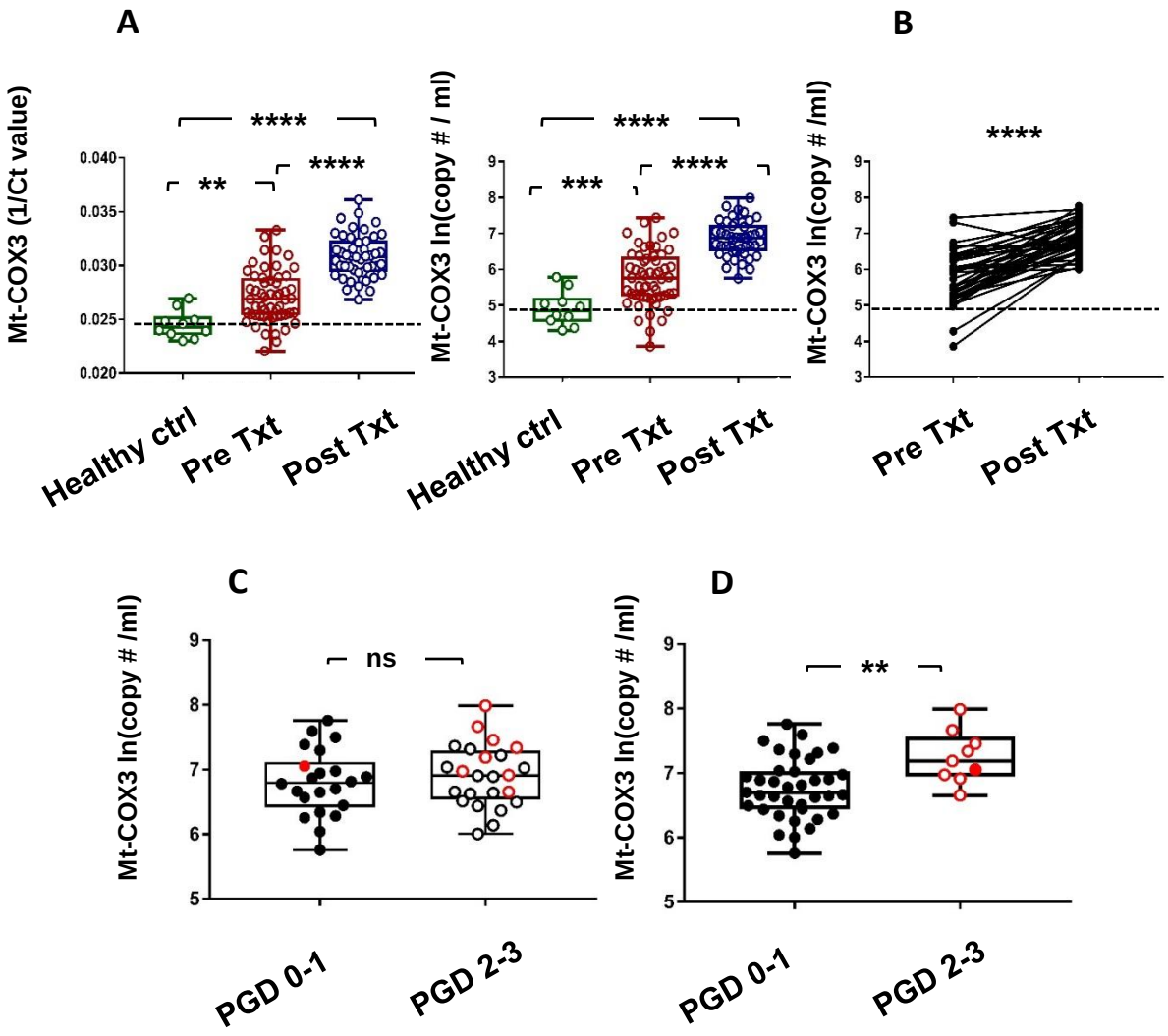

Supp. Fig. 4.2 Human lung recipients with PGD have elevated circulating Mt-DNA

(A) Box and whiskers plot of circulating Mt-COX3 DNA levels obtained from lung recipients within 6 to 12 hours after ICU arrival. (**p< 0.01, ****p< 0.0001). **(B)** Paired analysis plot of Mt-CYTB DNA levels for each patient before and after LTx (****p<0.0001). Dashed line represents the threshold limit for Mt-DNA detection (background). Box and whiskers plot of circulating Mt-COX3 DNA levels measured in lung recipients with PGD 0-1 or PGD 2-3 graded at (**C**) time 0 (upon arrival at the ICU) and (**D**) 72 hrs after ICU arrival (**p< 0.01). Open red circles are patients who persisted with PGD 2-3 from time 0 to 72 hrs. The filled red dot represents a patient whose PGD worsened from PGD 1 at time 0 to PGD 3 at 72 hours.

5. Discussion

PGD is an acute multifactorial syndrome which significantly increases morbidity and mortality after LTx and is associated with impaired recovery of the pulmonary function and increased risk of chronic rejection [4]. Although the underlying pathophysiological mechanisms of PGD remain obscure there is a general consensus that it is worsened by IRI resulting from either graft retrieval, preservation or implantation [1]. IRI can lead to tissue necrosis and release of a heterogeneous class of nuclear and cytosolic molecules, normally sequestered away from the immune system and collectively referred to as DAMPs [52]. DAMPs recognition by PRRs results in leukocyte activation and regulates their trafficking into the injured graft [125].

Several reports have shown that DAMPs are elevated in PGD and are associated to worsen ALI. These include high mobility group box 1 (HMGB1) [126], extracellular ATP [62] the soluble receptor for advanced glycation end products [127]. However, it remains unclear from these studies what is the exact contribution of DAMPs release in activating the recipient immune response which exacerbates PGD. In this regard, neutrophils are the most abundant cell infiltrating the graft early after transplant and several reports suggest that they may play a detrimental role in exacerbating tissue injury associated with ischemia reperfusion trough protease degranulation, release of proinflammatory cytokines and ROS burst [128]. Recent evidence indicates that a novel class of DAMPs originating from mitochondria and named Mt-DAMPs play a major contribution in neutrophil trafficking and activation in different models of sterile injury [69, 89].

Based on observations from a physiologically relevant model of syngeneic orthotopic LTx, we demonstrated that IRI promotes the intragraft release of donor-derived Mt-DAMPs. To our knowledge, this is the first direct evidence *in vivo* supporting the idea that LTx related ALI is associated with the release of Mt-DAMPs. Using transgenic mice, expressing mitochondrial-specific dendra2 fluorescent protein, we demonstrated that the donor graft is the predominant source of mitochondria release. Previous studies clearly demonstrated that graft cold preservation is associated with increased necrotic cell death which typically leads to the release of pro-inflammatory signals including Mt-DAMPs [129]. In addition, a recent work on kidney transplantation described the activation of a specific form of TNF-α-induced RIP1/3 dependent programmed necrosis named necroptosis [130]. In this regard, TNFα-induced necroptotic cells have been shown to directly release cell-free mitochondria [131]. Even if the role of necroptosis has not been yet investigated in LTx, our findings suggest that this specific program of cell death may be not restricted to kidney transplant. Interestingly, we also detected a small fraction of recipient-derived mitochondria. IRI is widely recognized as a bimodal process where an early phase, dominated by the ischemic metabolic alterations precedes reperfusion damage mostly dependent on immune cell activation [22]. From this prospective, the presence of recipient-derived mitochondria in damaged airways may represent the early immune response to the injured graft.

Increased circulating Mt-DAMPs have been associated with systemic inflammatory effects [69]. However, less is known about how they directly control local immune responses to damaged organs. Recent work has suggested that Mt-DAMPs-FPR1 axis guides neutrophils to focal areas of tissue injury suggesting that FPR1 acts as a necrotactic receptor [89]. However, the role of the Mt-DAMPs-FPR1 axis in regulating responses to

diffuse tissue damage after LTx is unclear. In addition, FPR1 can be expressed by non-immune cells [132] whose contribution to neutrophil behavior in response to Mt-DAMPs remains controversial [133]. To this end, the use of a solid organ transplant model of injury represents a unique tool offering the possibility to weight the relative contribution deployed by the donor graft cells compared to the recipient-derived immune cells to the IRI. Accordingly, we were able to dissect the role of FPR1 in neutrophil trafficking and lung injury by utilizing transplant combinations where either the recipient or the donor were FPR1 deficient. Unlike B6 or $FPR1^{-/-}$ recipients receiving B6 grafts, no significant differences were observed in airway neutrophilia, lung edema and vascular permeability in B6 recipients receiving either B6 or $FPR1^{-/-}$ grafts. This data suggest that FPR1 expression within donor-derived graft cell compartment doesn`t play a significant role in regulating neutrophil trafficking and consequent lung injury. However, FPR1 may also be expressed by other immune cells which can regulate neutrophil trafficking, such as monocytes [124, 134]. Here, we demonstrated that the abundance of infiltrating monocytes in graft tissue was comparable between B6 and $FPR1^{-/-}$ recipients of B6 lungs suggesting that neutrophil trafficking is independent of other infiltrating cells. Moreover, the intragraft accumulation of critical neutrophil chemoattractants released by activated monocytes such as CXCL1, CXCL2 and CXCL5, was comparable irrespective of FPR1 expression. Previous works using this LTx model have shown that neutrophil depletion or the inability to mobilize neutrophils attenuates LTx-mediated IRI [135, 136]. Therefore, taken together these data support the hypothesis that the expression of the Mt-DAMPs receptor FPR1 on the recipient-derived neutrophils contribute to the airway neutrophilia and the ALI observed after LTx.

Surprisingly, despite the significant difference observed in airway neutrophilia in the FPR1 recipients, the total level of neutrophil entry into the graft tissue and the rate of transendothelial migration remained comparable in all the different combination of LTx. This data suggest that FPR1 plays a role in neutrophil migration specifically in the extravascular compartment regulating intragraft neutrophil distribution.

Neutrophil trafficking into an injured organ is a complex and dynamic process [137]. Despite recent advances in elucidating the underlying mechanisms of neutrophil extravasation, less is known about neutrophil trafficking dynamics within interstitial tissues. Using 2-photon intravital imaging we have previously demonstrated the generation of extravascular neutrophil clusters in ischemically injured lung grafts [124]. However, it remains to be determined if neutrophil clusters may be regulated by the Mt-DAMPs-FPR1 axis. To our knowledge, here we provide the first direct evidence supporting that Mt-DAMPs contribute to neutrophil cluster formation. In addition, in our mouse model of LTx related IRI, we observed that $FPR1^{-/-}$ neutrophil clusters are significantly less stable compared to the littermate control. In this regard, Lammerman et al. recently show that, in a mouse model of laser-induced skin injury, FPR2 and not FPR1 is important to control neutrophil clusters [90] . Moreover, using a different model of sterile skin injury Liu et al. suggested that either FPR1 or FPR2 single deficiency is not sufficient to regulate early neutrophil accumulation [138]. Our findings consistently support the role of Mt-DAMPs in regulating neutrophil migration. However, in contrast with these reports, we demonstrated that FPR1 is sufficient to control neutrophil extravascular accumulation and cluster stability. Although the reasons for these differences are not clear it is possible that the role of FPR1 in neutrophil extravascular accumulation and cluster stability may be

injury or organ specific. Both of the earlier conclusions are predicated from observations around a single focal injury. IRIs in many organs, including the lung, are diffuse injuries and therefore are likely to generate a more complex environment where neutrophils encounter multiple and competing chemoattractant gradients from neighboring necrotic foci. In this scenario, the short-range effect described for the FPR1 dependent migration may play a more predominant role in controlling neutrophil trafficking in the area of injury. Thus the loss of FPR1 could make neutrophils more prone to multiple and dynamic chemotactic gradients generating continuous but poorly oriented motion. In contrast, in a model of focal damage, even in the absence of FPR1, no other confounding signals can distract the directional migration of neutrophil to the area of injury. Finally, the lung provides a unique framework for leukocyte migration since it is characterized by the presence of a peculiar compartment represented by the airways. In this regard, when we firstly analyzed leukocyte accumulation in the graft tissue we didn`t find any significant difference in neutrophil accumulation in the $FPR1^{-/-}$ compared to the B6. Our data, in fact, suggest that FPR1 specifically play a role in airway neutrophilia likely promoting neutrophil aggregation in clusters and consequent retention into the airways that, in virtue of the increased permeability, would represent a natural reservoir for a high concentration of Mt-DAMPs. An increased retention in an area rich of chemoattractant would be consistent with the intravital observations of the reduced interstitial velocity of the B6 neutrophils compared to the $FPR1^{-/-}$ which indicates a role for FPR1 in slow down cell migration in the presence of Mt-DAMPs.

Taken together these observations suggest a new paradigm for Mt-DAMPs-FPR1 axis besides the well-described role in promoting neutrophil migration in the site of injury.

With this thesis, we propose that the different intragraft distribution observed in the FPR1$^{-/-}$ recipients after LTx is not just the result of reduced neutrophil migration to the injured area but it is also related to a reduced neutrophil dwelling into the damaged airways associated to a fast motion behavior and to a cluster instability. Accordingly, we not just demonstrated that B6 airway neutrophils were significantly more abundant but also that they tend to remain in the airways for a longer period of time when compared to FPR1$^{-/-}$ neutrophils. Noting reports that suggest that neutrophil cluster required the expression of integrins at the site of cell death [119] and that the expression of CD11b is critical to regulate neutrophil velocity and dwelling time in glomerular space [139] we ask if Mt-DAMPs-FPR1 axis may be involved in regulating the expression of adhesion molecules on neutrophils. Our findings suggest that Mt-DAMPs are capable to induce a strong upregulation of neutrophil CD11b and that this effect is significantly reduced in FPR1$^{-/-}$ neutrophils. This data is consistent with previous observations suggesting that synthetic ligand of FPR1 are able to increase the expression of CD11b in neutrophil [140]. In addition, we tested the *in vitro* contribution of CD11b in the stability of neutrophil clusters formed in response to Mt-DAMPs stimulation. As expected, neutrophil cluster treated with the neutralizing Ab for CD11b exhibited a reduced size if compared to neutrophil cluster treated with isotype control. This data suggest that CD11b expression contributes to cluster stability by increasing neutrophils adhesiveness which, in turn, facilitates cell-cell stable interactions. A limit of this study is the lack of observations *in vivo* regarding the effect of CD11b blockade on cluster stability. However, CD11b expression plays a major role in different steps of neurophil migration especially in the transition from the rolling to the adhesive phase [112]. Either the use of a deficient mouse or the treatment with a

neutralizing Ab for CD11b would likely have a significant impact on the mechanisms of neutrophil intravascular migration making hard to understand the significance of the observation in the extravascular compartment.

Airways neutrophilia is generally considered a marker of ALI [47] and the graft tissue damage induced by ischemia-reperfusion is predominantly characterized by intra-alveolar leukocyte infiltration associated with alveolar wall injury [141]. In this regard, recent evidence shows that infiltrating neutrophils slow down their migration in nonperfused area after IRI [93] and that their prolonged retention is associated with an increased oxidative burst [139]. Here, we asked whether the peculiar intragraft neutrophil trafficking observed in the $FPR1^{-/-}$ recipients is associated with a different extension in the LTx-related ALI. The reduced lung edema and reduced vascular permeability along with the milder histological alteration observed in the $FPR1^{-/-}$ compared to the B6 support the hypothesis that FPR1 expression in the recipient but not in the donor cells contribute to exacerbate LTx-related ALI. P/F ratio is frequently used as a sign of reduced pulmonary functionality and is one of the criteria for the definition of PGD in humans. However, oxygenation is directly related to the availability of functioning lung tissue able to provide gas exchange. In mice, the right lung consists of 5 lobes compared to the left lung where only one lobe exist. The left lung contribution to the mouse Total Lung Capacity (TLC) is therefore very limited. For this reason, in our model of left orthotopic LTx, the larger contribution of the right respiratory system from the recipient is able to compensate a possible reduction in P/F ratio. However, lung edema, consisting in the increased content of water in the respiratory system, by definition represent a huge impairment to gas exchange and indirectly may support the idea that FPR1 may contribute to exacerbate PGD.

PGD is the clinical correlate of the early lung graft injury. Despite recent improvements in organ preservation, surgical technique, and perioperative care, PGD still represents a limitation to better short and long-term outcomes following LTx [2, 11]. Some donor and recipient clinical characteristics are commonly associated with the development and persistence of PGD [15, 16] However, despite several studies, no biomarker is currently available for clinical use in PGD [142]. In a recent study from Dorward et al. increased levels of formylated peptides have been measured in the BAL and serum of 10 ventilated patients affected by ARDS compared to healthy volunteers [92]. Moreover, circulating Mt-DNA levels have been found increased in several condition characterized by necrotic cell death such as trauma [143], acetaminophen hepatotoxicity [144] and coronary heart disease [75]. The levels of circulating Mt-DNA have also been demonstrated to correlate with clinical outcome in ICU patients with sepsis [76]. As previously discussed, necrotic cell death is an expected occurrence following LTx [129] which may justify the release of Mt-DAMPs. Therefore, based on the observations from our orthotopic LTx model, we investigated the role of Mt-DAMPs in our LTx recipient population. Using Mt-DNA as a surrogate marker, we measured circulating Mt-DAMPs in LTx recipients and healthy human volunteers. When compared to healthy volunteers, LTx recipients with or without PGD had significantly higher circulating Mt-DAMPs regardless the original indication to transplant. This observation suggests that the LTx procedure itself is capable to induce the release of Mt-DAMPs. However, LTx patients with moderate to severe PGD ($PaO_2/FiO_2 \leq 300$ mmHg) had significantly higher levels of circulating Mt-DAMPs than mild PGD ($PaO_2/FiO_2 > 300$ mmHg) upon arrival at the ICU (immediate-early PGD). Interestingly, many patients with immediate early PGD and higher levels of

Mt-DNA went to have moderate to severe PGD at 72 hours post-transplant suggesting that an early increase in Mt-DAMPs is associated with the persistence of lung function impairment. Severe PGD (grade 3) is generally considered to be different from other PGD grades and its occurrence, especially at 72 hours, has been related to worse clinical outcomes [5]. Although a limitation of our study is the small number of PGD3 patients observed after 72 hours, we found a significant early Mt-DAMPs increase in most of the patients with impaired lung function (P/F ratio $\leq$300) which include also patients with moderate PGD (grade 2). In this prospective, our observation of persistent impaired lung function in patients with early higher Mt-DAMPs seems to confirm the physiopathological role that these proinflammatory mediators exert in promoting ALI.

In conclusion, according to their association with persistent human ALI and based on the physiopathological role described in the animal model, Mt-DAMPs appear to be an excellent candidate as a prognostic biomarker for PGD severity after LTx. Future studies, based on larger series, may eventually assess a definitive role for Mt-DAMPs in this contest.

6. Bibliography

1. de Perrot, M., et al., *Ischemia-reperfusion-induced lung injury.* Am J Respir Crit Care Med, 2003. **167**(4): p. 490-511.
2. Christie, J.D., et al., *Impact of primary graft failure on outcomes following lung transplantation.* Chest, 2005. **127**(1): p. 161-5.
3. Khan, S.U., et al., *Acute pulmonary edema after lung transplantation: the pulmonary reimplantation response.* Chest, 1999. **116**(1): p. 187-94.
4. Christie, J.D., et al., *Report of the ISHLT Working Group on Primary Lung Graft Dysfunction part II: definition. A consensus statement of the International Society for Heart and Lung Transplantation.* J Heart Lung Transplant, 2005. **24**(10): p. 1454-9.
5. Christie, J.D., et al., *Construct validity of the definition of primary graft dysfunction after lung transplantation.* J Heart Lung Transplant, 2010. **29**(11): p. 1231-9.
6. Diamond, J.M., et al., *Clinical risk factors for primary graft dysfunction after lung transplantation.* Am J Respir Crit Care Med, 2013. **187**(5): p. 527-34.
7. Prekker, M.E., et al., *Validation of the proposed International Society for Heart and Lung Transplantation grading system for primary graft dysfunction after lung transplantation.* J Heart Lung Transplant, 2006. **25**(4): p. 371-8.
8. Kreisel, D., et al., *Short- and long-term outcomes of 1000 adult lung transplant recipients at a single center.* J Thorac Cardiovasc Surg, 2011. **141**(1): p. 215-22.
9. Daud, S.A., et al., *Impact of immediate primary lung allograft dysfunction on bronchiolitis obliterans syndrome.* Am J Respir Crit Care Med, 2007. **175**(5): p. 507-13.
10. Huang, H.J., et al., *Late primary graft dysfunction after lung transplantation and bronchiolitis obliterans syndrome.* Am J Transplant, 2008. **8**(11): p. 2454-62.
11. Whitson, B.A., et al., *Primary graft dysfunction and long-term pulmonary function after lung transplantation.* J Heart Lung Transplant, 2007. **26**(10): p. 1004-11.
12. Christie, J.D., et al., *The effect of primary graft dysfunction on survival after lung transplantation.* Am J Respir Crit Care Med, 2005. **171**(11): p. 1312-6.
13. Arcasoy, S.M., et al., *Report of the ISHLT Working Group on Primary Lung Graft Dysfunction part V: predictors and outcomes.* J Heart Lung Transplant, 2005. **24**(10): p. 1483-8.
14. Shah, R.J., et al., *Early plasma soluble Receptor for Advanced Glycation End Product levels are associated with bronchiolitis obliterans syndrome.* American journal of transplantation : official journal of the American Society of Transplantation and the American Society of Transplant Surgeons, 2013. **13**(3): p. 754-759.
15. Whitson, B.A., et al., *Risk factors for primary graft dysfunction after lung transplantation.* J Thorac Cardiovasc Surg, 2006. **131**(1): p. 73-80.
16. Christie et al., *Christie et al., 2003.*
17. Barr, M.L., et al., *Report of the ISHLT Working Group on Primary Lung Graft Dysfunction part IV: recipient-related risk factors and markers.* J Heart Lung Transplant, 2005. **24**(10): p. 1468-82.
18. Fang, A., et al., *Elevated pulmonary artery pressure is a risk factor for primary graft dysfunction following lung transplantation for idiopathic pulmonary fibrosis.* Chest, 2011. **139**(4): p. 782-787.

19. Avlonitis, V.S., et al., *Early hemodynamic injury during donor brain death determines the severity of primary graft dysfunction after lung transplantation.* Am J Transplant, 2007. **7**(1): p. 83-90.
20. *Dreyfuss et al., 1995.*
21. Akhtar et al., *Novel approaches to preventing ischemia-reperfusion injury during liver transplantation.* Transplant Proc, 2013. **45**(6): p. 2083-92.
22. Kalogeris et al., *Cell biology of ischemia/reperfusion injury.* Int Rev Cell Mol Biol, 2012. **298**: p. 229-317.
23. Granger, D.N. and P.R. Kvietys, *Reperfusion injury and reactive oxygen species: The evolution of a concept.* Redox Biol, 2015. **6**: p. 524-51.
24. Brookes et al., *Calcium, ATP, and ROS: a mitochondrial love-hate triangle.* Am J Physiol Cell Physiol, 2004. **287**(4): p. C817-33.
25. Wang et al., *Poly(ADP-ribose) Signals to Mitochondrial AIF: A Key Event in Parthanatos.* Experimental neurology, 2009. **218**(2): p. 193-202.
26. Girn et al., *Reperfusion syndrome: cellular mechanisms of microvascular dysfunction and potential therapeutic strategies.* Vasc Endovascular Surg, 2007. **41**(4): p. 277-93.
27. Taylor, A.E., *Pulmonary edema: ischemia reperfusion endothelial injury and its reversal by c-AMP.* Proc Natl Sci Counc Repub China B, 1991. **15**(3): p. 191-5.
28. Eppinger et al., *Pattern of Injury and the Role of Neutrophils in Reperfusion Injury of Rat Lung.* Journal of Surgical Research, 1995. **58**(6): p. 713-718.
29. Zheng, L., et al., *The dynamics and associations of airway neutrophilia post lung transplantation.* Am J Transplant, 2006. **6**(3): p. 599-608.
30. Diamond et al., *Role of innate immunity in primary graft dysfunction after lung transplantation.* Curr Opin Organ Transplant, 2013. **18**(5): p. 518-23.
31. Sayah, D.M., et al., *Neutrophil extracellular traps are pathogenic in primary graft dysfunction after lung transplantation.* Am J Respir Crit Care Med, 2015. **191**(4): p. 455-63.
32. Hemmert, C., et al., *Imaging of lung transplant complications.* Diagn Interv Imaging, 2014. **95**(4): p. 399-409.
33. Anderson et al.
34. Suzuki, Y., E. Cantu, and J.D. Christie, *Primary Graft Dysfunction.* Seminars in respiratory and critical care medicine, 2013. **34**(3): p. 305-319.
35. Altun, G.T., M.K. Arslantaş, and İ. Cinel, *Primary Graft Dysfunction after Lung Transplantation.* Turkish Journal of Anaesthesiology and Reanimation, 2015. **43**(6): p. 418-423.
36. Shargall, Y., et al., *Report of the ISHLT Working Group on Primary Lung Graft Dysfunction Part VI: Treatment.* The Journal of Heart and Lung Transplantation, 2005. **24**(10): p. 1489-1500.
37. Meyers, B.F., et al., *Selective use of extracorporeal membrane oxygenation is warranted after lung transplantation.* The Journal of Thoracic and Cardiovascular Surgery, 2000. **120**(1): p. 20-28.
38. Hartwig, M.G., et al., *Improved Survival but Marginal Allograft Function in Patients Treated With Extracorporeal Membrane Oxygenation After Lung Transplantation.* The Annals of Thoracic Surgery, 2012. **93**(2): p. 366-371.
39. de Perrot, M., et al., *Report of the ISHLT Working Group on Primary Lung Graft Dysfunction Part III: Donor-Related Risk Factors and Markers.* The Journal of Heart and Lung Transplantation, 2005. **24**(10): p. 1460-1467.

40. Venuta, F., et al., *Preimplantation retrograde pneumoplegia in clinical lung transplantation.* J Thorac Cardiovasc Surg, 1999. **118**(1): p. 107-14.
41. Dos Santos, C.C. and A.S. Slutsky, *Invited review: mechanisms of ventilator-induced lung injury: a perspective.* J Appl Physiol (1985), 2000. **89**(4): p. 1645-55.
42. McRae, K.M., *Pulmonary transplantation.* Curr Opin Anaesthesiol, 2000. **13**(1): p. 53-9.
43. Pierre, A.F., et al., *Rapid reperfusion causes stress failure in ischemic rat lungs.* J Thorac Cardiovasc Surg, 1998. **116**(6): p. 932-42.
44. Halldorsson, A., et al., *Controlled reperfusion after lung ischemia: implications for improved function after lung transplantation.* J Thorac Cardiovasc Surg, 1998. **115**(2): p. 415-24; discussion 424-5.
45. Bhabra, M.S., et al., *Controlled reperfusion protects lung grafts during a transient early increase in permeability.* Ann Thorac Surg, 1998. **65**(1): p. 187-92.
46. Fischer, S., et al., *In vivo donor adenoviral-mediated transtracheal transfection of human IL-10 (HIL-10) gene ameliorates ischemia-reperfusion (IR) injury and enhances transplanted lung function.* J Heart Lung Transplant, 2001. **20**(2): p. 152-153.
47. Grommes, J. and O. Soehnlein, *Contribution of neutrophils to acute lung injury.* Mol Med, 2011. **17**(3-4): p. 293-307.
48. Nathan et al., *Neutrophils and immunity: challenges and opportunities.* Nat Rev Immunol, 2006. **6**(3): p. 173-82.
49. Yang, C.W., et al., *Neutrophils influence the level of antigen presentation during the immune response to protein antigens in adjuvants.* J Immunol, 2010. **185**(5): p. 2927-34.
50. Matzinger, P., *The evolution of the danger theory.* Expert review of clinical immunology, 2012. **8**(4): p. 311-317.
51. Vénéreau, E., C. Ceriotti, and M.E. Bianchi, *DAMPs from Cell Death to New Life.* Frontiers in Immunology, 2015. **6**: p. 422.
52. Braza, F., et al., *Role of TLRs and DAMPs in allograft inflammation and transplant outcomes.* Nat Rev Nephrol, 2016. **12**(5): p. 281-90.
53. Mogensen, T.H., *Pathogen Recognition and Inflammatory Signaling in Innate Immune Defenses.* Clinical Microbiology Reviews, 2009. **22**(2): p. 240-273.
54. Braza, F., et al., *Role of TLRs and DAMPs in allograft inflammation and transplant outcomes.* Nat Rev Nephrol, 2016. **advance online publication**.
55. Ding, H.S., et al., *The HMGB1-TLR4 axis contributes to myocardial ischemia/reperfusion injury via regulation of cardiomyocyte apoptosis.* Gene, 2013. **527**(1): p. 389-93.
56. Chen, C.B., et al., *Up-Regulation of HMGB1 Exacerbates Renal Ischemia-Reperfusion Injury by Stimulating Inflammatory and Immune Responses through the TLR4 Signaling Pathway in Mice.* Cell Physiol Biochem, 2017. **41**(6): p. 2447-2460.
57. Zhao, G., et al., *Down-regulation of nuclear HMGB1 reduces ischemia-induced HMGB1 translocation and release and protects against liver ischemia-reperfusion injury.* Sci Rep, 2017. **7**: p. 46272.
58. Weber, D.J., et al., *The HMGB1-RAGE axis mediates traumatic brain injury-induced pulmonary dysfunction in lung transplantation.* Sci Transl Med, 2014. **6**(252): p. 252ra124.
59. Mersmann, J., et al., *Attenuation of Myocardial Injury by HMGB1 Blockade during Ischemia/Reperfusion Is Toll-Like Receptor 2-Dependent.* Mediators of Inflammation, 2013. **2013**: p. 174168.
60. McDonald, K.A., et al., *Toll-like receptor 4 (TLR4) antagonist eritoran tetrasodium attenuates liver ischemia and reperfusion injury through inhibition of high-mobility group box protein B1 (HMGB1) signaling.* Mol Med, 2015. **20**: p. 639-48.

61. Ibrahim, M., et al., *Human Recombinant Apyrase Therapy Protects Against Canine Pulmonary Ischemia-Reperfusion Injury.* The Journal of heart and lung transplantation : the official publication of the International Society for Heart Transplantation, 2015. **34**(2): p. 247-253.
62. Sugimoto, S., et al., *Apyrase treatment prevents ischemia-reperfusion injury in rat lung isografts.* J Thorac Cardiovasc Surg, 2009. **138**(3): p. 752-9.
63. Wu, H., et al., *TLR4 activation mediates kidney ischemia/reperfusion injury.* J Clin Invest, 2007. **117**(10): p. 2847-59.
64. Jiang, D., J. Liang, and P.W. Noble, *Hyaluronan as an immune regulator in human diseases.* Physiol Rev, 2011. **91**(1): p. 221-64.
65. Todd, J.L., et al., *Hyaluronan contributes to bronchiolitis obliterans syndrome and stimulates lung allograft rejection through activation of innate immunity.* Am J Respir Crit Care Med, 2014. **189**(5): p. 556-66.
66. Zhang, Q., et al., *Circulating mitochondrial DAMPs cause inflammatory responses to injury.* Nature, 2010. **464**(7285): p. 104-7.
67. Eleftheriadis, T., et al., *Cytochrome c as a Potentially Clinical Useful Marker of Mitochondrial and Cellular Damage.* Frontiers in Immunology, 2016. **7**(279).
68. Nakahira, K., S. Hisata, and A.M.K. Choi, *The Roles of Mitochondrial Damage-Associated Molecular Patterns in Diseases.* Antioxidants & Redox Signaling, 2015. **23**(17): p. 1329-1350.
69. Zhang, Q., et al., *Circulating Mitochondrial DAMPs Cause Inflammatory Responses to Injury.* Nature, 2010. **464**(7285): p. 104-107.
70. Takeshita, F., et al., *Signal transduction pathways mediated by the interaction of CpG DNA with Toll-like receptor 9.* Seminars in Immunology, 2004. **16**(1): p. 17-22.
71. Rao, H., et al., *Correlation between TLR9 Expression and Cytokine Secretion in the Clinical Diagnosis of Systemic Lupus Erythematosus.* Mediators Inflamm, 2015. **2015**: p. 710720.
72. Chen, L., et al., *TLR engagement prevents transplantation tolerance.* Am J Transplant, 2006. **6**(10): p. 2282-91.
73. Puskarich, M.A., et al., *Plasma levels of mitochondrial DNA in patients presenting to the emergency department with sepsis.* Shock, 2012. **38**(4): p. 337-40.
74. Rodrigues Filho, E.M., et al., *Prognostic value of circulating DNA levels in critically ill and trauma patients.* Revista Brasileira de Terapia Intensiva, 2014. **26**(3): p. 305-312.
75. Liu, J., et al., *Circulating Cell Free Mitochondrial DNA is a Biomarker in the Development of Coronary Heart Disease in the Patients with Type 2 Diabetes.* Clin Lab, 2015. **61**(7): p. 661-7.
76. Nakahira, K., et al., *Circulating mitochondrial DNA in patients in the ICU as a marker of mortality: derivation and validation.* PLoS Med, 2013. **10**(12): p. e1001577; discussion e1001577.
77. Wenceslau, C.F., et al., *Mitochondrial-derived N-formyl peptides: novel links between trauma, vascular collapse and sepsis.* Med Hypotheses, 2013. **81**(4): p. 532-5.
78. RajBhandary, U.L., *Initiator transfer RNAs.* J Bacteriol, 1994. **176**(3): p. 547-52.
79. Spencer, A.C. and L.L. Spremulli, *Interaction of mitochondrial initiation factor 2 with mitochondrial fMet-tRNA.* Nucleic Acids Research, 2004. **32**(18): p. 5464-5470.
80. Dorward, D.A., et al., *The Role of Formylated Peptides and Formyl Peptide Receptor 1 in Governing Neutrophil Function during Acute Inflammation.* The American Journal of Pathology, 2015. **185**(5): p. 1172-1184.
81. Calfee, C.S. and M.A. Matthay, *Clinical immunology: Culprits with evolutionary ties.* Nature, 2010. **464**(7285): p. 41-2.

82. Dufton, N. and M. Perretti, *Therapeutic anti-inflammatory potential of formyl-peptide receptor agonists.* Pharmacology & Therapeutics, 2010. **127**(2): p. 175-188.
83. Rabiet, M.-J., E. Huet, and F. Boulay, *The N-formyl peptide receptors and the anaphylatoxin C5a receptors: An overview.* Biochimie, 2007. **89**(9): p. 1089-1106.
84. Ye, R.D., et al., *International Union of Basic and Clinical Pharmacology. LXXIII. Nomenclature for the formyl peptide receptor (FPR) family.* Pharmacol Rev, 2009. **61**(2): p. 119-61.
85. Bao, L., et al., *Mapping of genes for the human C5a receptor (C5AR), human FMLP receptor (FPR), and two FMLP receptor homologue orphan receptors (FPRH1, FPRH2) to chromosome 19.* Genomics, 1992. **13**(2): p. 437-440.
86. Sengelov, H., et al., *Subcellular localization and translocation of the receptor for N-formylmethionyl-leucyl-phenylalanine in human neutrophils.* Biochem J, 1994. **299 (Pt 2)**: p. 473-9.
87. O'Flaherty, J.T., et al., *Tumor necrosis factor-alpha regulates expression of receptors for formyl-methionyl-leucyl-phenylalanine, leukotriene B4, and platelet-activating factor. Dissociation from priming in human polymorphonuclear neutrophils.* J Immunol, 1991. **147**(11): p. 3842-7.
88. Gao, J.-L., et al., *Differential Expansion of the N-Formylpeptide Receptor Gene Cluster in Human and Mouse.* Genomics, 1998. **51**(2): p. 270-276.
89. McDonald, B., et al., *Intravascular danger signals guide neutrophils to sites of sterile inflammation.* Science, 2010. **330**(6002): p. 362-6.
90. Lammermann, T., et al., *Neutrophil swarms require LTB4 and integrins at sites of cell death in vivo.* Nature, 2013. **498**(7454): p. 371-5.
91. Cardini, S., et al., *Genetic ablation of the fpr1 gene confers protection from smoking-induced lung emphysema in mice.* Am J Respir Cell Mol Biol, 2012. **47**(3): p. 332-9.
92. Dorward, D.A., et al., *Novel role for endogenous mitochondrial formylated peptide-driven formyl peptide receptor 1 signalling in acute respiratory distress syndrome.* Thorax, 2017. **72**(10): p. 928-936.
93. Honda, M., et al., *Intravital Imaging of Neutrophil Recruitment Reveals the Efficacy of FPR1 Blockade in Hepatic Ischemia-Reperfusion Injury.* J Immunol, 2017. **198**(4): p. 1718-1728.
94. Schepetkin, I.A., et al., *Antagonism of human formyl peptide receptor 1 with natural compounds and their synthetic derivatives.* International Immunopharmacology, 2016. **37**: p. 43-58.
95. Summers, C., et al., *Neutrophil kinetics in health and disease.* Trends in Immunology, 2010. **31**(8): p. 318-324.
96. Dahl, R., et al., *Regulation of macrophage and neutrophil cell fates by the PU.1:C/EBPalpha ratio and granulocyte colony-stimulating factor.* Nat Immunol, 2003. **4**(10): p. 1029-36.
97. Borregaard, N., *Neutrophils, from Marrow to Microbes.* Immunity, 2010. **33**(5): p. 657-670.
98. Lieschke, G.J., et al., *Mice lacking granulocyte colony-stimulating factor have chronic neutropenia, granulocyte and macrophage progenitor cell deficiency, and impaired neutrophil mobilization.* Blood, 1994. **84**(6): p. 1737-46.
99. Gaffen, S.L., et al., *IL-23-IL-17 immune axis: Discovery, Mechanistic Understanding, and Clinical Testing.* Nature reviews. Immunology, 2014. **14**(9): p. 585-600.
100. Stark, M.A., et al., *Phagocytosis of apoptotic neutrophils regulates granulopoiesis via IL-23 and IL-17.* Immunity, 2005. **22**(3): p. 285-94.

101. Kreisel, D., et al., *Emergency granulopoiesis promotes neutrophil-dendritic cell encounters that prevent mouse lung allograft acceptance.* Blood, 2011. **118**(23): p. 6172-82.
102. Faurschou, M. and N. Borregaard, *Neutrophil granules and secretory vesicles in inflammation.* Microbes Infect, 2003. **5**(14): p. 1317-27.
103. Borregaard, N., O.E. Sorensen, and K. Theilgaard-Monch, *Neutrophil granules: a library of innate immunity proteins.* Trends Immunol, 2007. **28**(8): p. 340-5.
104. Lacy, P., *Mechanisms of Degranulation in Neutrophils.* Allergy, Asthma, and Clinical Immunology : Official Journal of the Canadian Society of Allergy and Clinical Immunology, 2006. **2**(3): p. 98-108.
105. Underhill, D.M. and A. Ozinsky, *Phagocytosis of microbes: complexity in action.* Annu Rev Immunol, 2002. **20**: p. 825-52.
106. Babior, B.M., J.D. Lambeth, and W. Nauseef, *The neutrophil NADPH oxidase.* Arch Biochem Biophys, 2002. **397**(2): p. 342-4.
107. Segal, A.W., *How neutrophils kill microbes.* Annu Rev Immunol, 2005. **23**: p. 197-223.
108. O'Neill, S., et al., *Genetic disorders coupled to ROS deficiency.* Redox Biology, 2015. **6**(Supplement C): p. 135-156.
109. Loukogeorgakis, S.P., et al., *Role of NADPH oxidase in endothelial ischemia/reperfusion injury in humans.* Circulation, 2010. **121**(21): p. 2310-6.
110. Hoffmeyer, M.R., et al., *Myocardial ischemia/reperfusion injury in NADPH oxidase-deficient mice.* Circ Res, 2000. **87**(9): p. 812-7.
111. Ovechkin, A.V., et al., *Lung ischemia-reperfusion injury: implications of oxidative stress and platelet-arteriolar wall interactions.* Arch Physiol Biochem, 2007. **113**(1): p. 1-12.
112. Wagner, J.G. and R.A. Roth, *Neutrophil Migration Mechanisms, with an Emphasis on the Pulmonary Vasculature.* Pharmacological Reviews, 2000. **52**(3): p. 349.
113. Lu, Y.T., P.G. Chen, and S.F. Liu, *Time course of lung ischemia-reperfusion-induced ICAM-1 expression and its role in ischemia-reperfusion lung injury.* J Appl Physiol (1985), 2002. **93**(2): p. 620-8.
114. Weninger, W., M. Biro, and R. Jain, *Leukocyte migration in the interstitial space of non-lymphoid organs.* Nat Rev Immunol, 2014. **14**(4): p. 232-246.
115. Kienle, K. and T. Lammermann, *Neutrophil swarming: an essential process of the neutrophil tissue response.* Immunol Rev, 2016. **273**(1): p. 76-93.
116. Ng, L.G., et al., *Visualizing the Neutrophil Response to Sterile Tissue Injury in Mouse Dermis Reveals a Three-Phase Cascade of Events.* Journal of Investigative Dermatology, 2011. **131**(10): p. 2058-2068.
117. Chtanova, T., et al., *Dynamics of Neutrophil Migration in Lymph Nodes during Infection.* Immunity, 2008. **29**(3): p. 487-496.
118. Afonso, Philippe V., et al., *LTB4 Is a Signal-Relay Molecule during Neutrophil Chemotaxis.* Developmental Cell, 2012. **22**(5): p. 1079-1091.
119. Lammermann, T., et al., *Neutrophil swarms require LTB4 and integrins at sites of cell death in vivo.* Nature, 2013. **498**(7454): p. 371-375.
120. Yusen, R.D., et al., *The Registry of the International Society for Heart and Lung Transplantation: Thirty-second Official Adult Lung and Heart-Lung Transplantation Report--2015; Focus Theme: Early Graft Failure.* J Heart Lung Transplant, 2015. **34**(10): p. 1264-77.
121. Braza, F., et al., *Role of TLRs and DAMPs in allograft inflammation and transplant outcomes.* Nat Rev Nephrol, 2016.

122. Hauser, C.J., et al., *Mitochondrial damage associated molecular patterns from femoral reamings activate neutrophils through formyl peptide receptors and P44/42 MAP kinase.* J Orthop Trauma, 2010. **24**(9): p. 534-8.
123. Krupnick, A.S., et al., *Orthotopic mouse lung transplantation as experimental methodology to study transplant and tumor biology.* Nat Protoc, 2009. **4**(1): p. 86-93.
124. Kreisel, D., et al., *In vivo two-photon imaging reveals monocyte-dependent neutrophil extravasation during pulmonary inflammation.* Proc Natl Acad Sci U S A, 2010. **107**(42): p. 18073-8.
125. Land, W.G., et al., *Transplantation and Damage-Associated Molecular Patterns (DAMPs).* Am J Transplant, 2016. **16**(12): p. 3338-3361.
126. Weber, D.J., et al., *The HMGB1-RAGE axis mediates traumatic brain injury–induced pulmonary dysfunction in lung transplantation.* Science Translational Medicine, 2014. **6**(252): p. 252ra124.
127. Christie, J.D., et al., *Plasma levels of receptor for advanced glycation end products, blood transfusion, and risk of primary graft dysfunction.* Am J Respir Crit Care Med, 2009. **180**(10): p. 1010-5.
128. Scozzi, D., et al., *The Role of Neutrophils in Transplanted Organs.* Am J Transplant, 2016.
129. Fischer, S., et al., *Dynamic changes in apoptotic and necrotic cell death correlate with severity of ischemia-reperfusion injury in lung transplantation.* Am J Respir Crit Care Med, 2000. **162**(5): p. 1932-9.
130. Lau, A., et al., *RIPK3-mediated necroptosis promotes donor kidney inflammatory injury and reduces allograft survival.* Am J Transplant, 2013. **13**(11): p. 2805-18.
131. Maeda, A. and B. Fadeel, *Mitochondria released by cells undergoing TNF-alpha-induced necroptosis act as danger signals.* Cell Death Dis, 2014. **5**: p. e1312.
132. Wenceslau, C.F., C.G. McCarthy, and R.C. Webb, *Formyl Peptide Receptor Activation Elicits Endothelial Cell Contraction and Vascular Leakage.* Front Immunol, 2016. **7**: p. 297.
133. Sun, S., et al., *Mitochondrial DAMPs increase endothelial permeability through neutrophil dependent and independent pathways.* PLoS One, 2013. **8**(3): p. e59989.
134. Crouser, E.D., et al., *Monocyte activation by necrotic cells is promoted by mitochondrial proteins and formyl peptide receptors.* Crit Care Med, 2009. **37**(6): p. 2000-9.
135. Belperio, J.A., et al., *CXCR2/CXCR2 ligand biology during lung transplant ischemia-reperfusion injury.* J Immunol, 2005. **175**(10): p. 6931-9.
136. Yamamoto, S., et al., *Cutting edge: Pseudomonas aeruginosa abolishes established lung transplant tolerance by stimulating B7 expression on neutrophils.* J Immunol, 2012. **189**(9): p. 4221-5.
137. Sanz, M.J. and P. Kubes, *Neutrophil-active chemokines in in vivo imaging of neutrophil trafficking.* Eur J Immunol, 2012. **42**(2): p. 278-83.
138. Liu, M., et al., *Formylpeptide receptors mediate rapid neutrophil mobilization to accelerate wound healing.* PLoS One, 2014. **9**(6): p. e90613.
139. Devi, S., et al., *Multiphoton imaging reveals a new leukocyte recruitment paradigm in the glomerulus.* Nat Med, 2013. **19**(1): p. 107-112.
140. Saito, Y., et al., *Adrenomedullin suppresses fMLP-induced upregulation of CD11b of human neutrophils.* Inflammation, 2001. **25**(3): p. 197-201.
141. Draenert, A., et al., *Ischaemia-reperfusion injury in orthotopic mouse lung transplants – a scanning electron microscopy study.* International Journal of Experimental Pathology, 2011. **92**(1): p. 18-25.

142. Calfee, C.S. and L.B. Ware, *Biomarkers of lung injury in primary graft dysfunction following lung transplantation.* Biomark Med, 2007. **1**(2): p. 285-91.
143. Lam, N.Y.L., et al., *Plasma Mitochondrial DNA Concentrations after Trauma.* Clinical Chemistry, 2004. **50**(1): p. 213.
144. McGill, M.R., et al., *Serum mitochondrial biomarkers and damage-associated molecular patterns are higher in acetaminophen overdose patients with poor outcome.* Hepatology (Baltimore, Md.), 2014. **60**(4): p. 1336-1345.

7. Acknowledgments

Firstly, I would like to express sincere gratitude to Prof. Salvatore Mariotta and to Prof. Andrew Gelman. Through their precious guidance and support they both greatly contributes to this research.

I thank all my fellow lab mates, in particular Dr. Hsiao Hsi-Min, for the technical support, the scientific discussions and in general for all the fun we have had in the lab.

Last but not the least, I would like to thank my parents (Mirella and Antonio), my brothers (Paolo and Stefano) and my fiancee Claudia that with extreme love and patience have always supported and encouraged me.